

# Establishing a Connection between Alzheimer's Disease and Cellular Energy Transduction



A

Major Qualifying Project Report

Submitted to the Faculty of

WORCESTER POLYTECHNIC INSTITUTE

In partial fulfillment of the requirements for the

Degree of Bachelor of Science

By:

Timothy Consedine

Lily Randle

Nathan McNeill

Approved by:

Professor Jagan Srinivasan

Professor Carissa Olsen

Worcester Polytechnic Institute

Biology and Biotechnology

Chemistry and Biochemistry

*This report represents the work of one or more WPI undergraduate students submitted to the faculty as evidence of completion of a degree requirement. WPI routinely publishes these reports on its web site without editorial or peer review.*

## **Acknowledgments**

We would like to thank Dr. Jagan Srinivasan, Dr. Carissa Perez Olsen, Douglas Reilly, Christopher Chute, and Elizabeth DiLoreto for their continued support and assistance throughout this project. We would also like to recognize Dr. Christopher Link at the University of Colorado, Boulder for developing the Alzheimer's' Disease transgenic model. All additional strains were obtained from the Caenorhabditis Genetic Center (CGC).

## Abstract

In the United States, prevalence of Alzheimer's Disease (AD) is rising, with an expected increase from 5.7 to 14 million patients by 2050. Characterized by the accumulation of amyloid-beta plaques in the brain, AD results in loss of cognitive and motor functions, with a theorized link to metabolism and ATP production. This study used transgenic AD-model and metabolic mutant *Caenorhabditis elegans* to investigate punicalagin and coenzyme Q<sub>10</sub> as possible treatments through behavioral and ATP-quantifying assays. Both treatments were successful in rescuing chemosensory ability in AD model and metabolic mutant strains. The ability to rescue both model systems with each treatment suggests a metabolic deficiency resulting in olfactory dysfunction. Punicalagin and coenzyme Q<sub>10</sub> rescued mobility in AD and *coq-3* worms, respectively.

# Table of Contents

Contents	
Acknowledgments	i
Abstract	ii
Table of Contents	iii
<b>1. Background</b>	<b>1</b>
<b>1.1 Metabolism and its role in disorder</b>	<b>1</b>
<b>1.1.1 Overview of Metabolism</b>	<b>1</b>
<b>1.1.2 The Electron Transport Chain</b>	<b>3</b>
<b>1.2: Metabolism and Neurodegeneration in Humans</b>	<b>7</b>
<b>1.2.1 Overview of Metabolic Disorders</b>	<b>7</b>
<b>1.2.2 Neurodegenerative Diseases and Metabolism</b>	<b>9</b>
<b>1.2.3 Metabolism in classic Neurodegenerative Disorders: Alzheimer’s Disease</b>	<b>10</b>
<b>1.2.4 Polyphenols in Therapeutics</b>	<b>13</b>
<b>1.3 <i>C. elegans</i> as a Model Organism</b>	<b>15</b>
<b>1.3.1 The Life Cycle of <i>C. elegans</i></b>	<b>15</b>
<b>1.3.2 <i>C. elegans</i> as a model for metabolic disorders</b>	<b>17</b>
<b>1.3.3 <i>C. elegans</i> as a model for AD</b>	<b>18</b>
<b>1.4 New Directions: Our Project Overview</b>	<b>19</b>
<b>2. Methodology</b>	<b>20</b>
<b>2.1 Worm Protocol</b>	<b>20</b>
<b>2.1.1 Maintenance</b>	<b>20</b>
<b>2.1.2 Strains</b>	<b>20</b>
<b>2.1.3 Heat Shock to Induce Mutations</b>	<b>22</b>
<b>2.2 Addition of Derivatives to LB media and OP50</b>	<b>22</b>
<b>2.2.1 Punicalagin</b>	<b>22</b>
<b>2.2.2 Coenzyme Q<sub>10</sub></b>	<b>23</b>
<b>2.3 Assays</b>	<b>23</b>
<b>2.3.1 Avoidance Assay</b>	<b>23</b>
<b>2.3.2 Chemotaxis Assay</b>	<b>25</b>

<b>2.3.3 Locomotion Assay</b>	26
<b>2.3.4 ATP Bioluminescence Assay</b>	27
<b>3. Results and Discussion</b>	30
<b>3.1 Baseline testing</b>	30
<b>3.1.1 Avoidance Assay</b>	30
<b>3.1.2 Chemotaxis Assay</b>	31
<b>3.1.3 Mobility Assay</b>	32
<b>3.1.4 ATP Bioluminescence Assay</b>	33
<b>3.2 Punicalagin Treatment</b>	34
<b>3.2.1 Avoidance Assay</b>	34
<b>3.2.2 Chemotaxis Assay</b>	36
<b>3.2.3 Mobility Assay</b>	37
<b>3.2.4 ATP Bioluminescence Assay</b>	38
<b>3.3 Coenzyme Q<sub>10</sub></b>	40
<b>3.3.1 Avoidance Assay</b>	40
<b>3.3.2 Chemotaxis Assay</b>	42
<b>3.3.3 Mobility Assay</b>	43
<b>3.3.4 ATP Bioluminescence Assay</b>	45
<b>4. Conclusions and Future Work</b>	48
<b>4.1 Conclusions</b>	48
<b>4.2 Future Work</b>	50
<b>Bibliography</b>	52

# 1. Background

## 1.1 Metabolism and its role in disorder

### 1.1.1 Overview of Metabolism

Metabolism is defined as all of the reactions that occur within an organism. Some of these reactions produce energy while others produce the building blocks of life such as amino acids, fatty acids, and nucleotides. The most active sites for metabolic process are located in the liver, brain, and muscles. Energy production is facilitated by digestion and the cellular processes involved in the breakdown of food and the processing and storage of metabolites. There are three stages that turn food into energy. The first stage is the breakdown of food through digestion, the intestines absorb it and then the circulatory system distributes it. The second stage occurs on the cellular level. Within the cells, simple sugars, lipids, fatty acids and amino acids are broken down into metabolites. This step subsequently produce a small amount of the cell's total energy (Wildman and Medeiros, 2015). The third step is when the metabolites produced in the second step are converted into carbon dioxide and water producing most of the cell's energy.

There are two types of metabolic pathways involved in the process by which organisms produce energy. These two different processes are known as catabolism and anabolism. Catabolism is the breakdown of large compounds into smaller ones while anabolism is the building of larger compounds from smaller ones. Metabolic pathways are never truly inactive since they produce important biological molecules in all cell types. The main energy producing organelle within most complex cell types is the mitochondrion (Wildman and Medeiros, 2015). This organelle has a variety of localized transmembrane complexes present that facilitate in the production of energy molecules such as adenosine triphosphate (ATP), nicotinamide adenine dinucleotide phosphate (NADPH), nicotinamide dinucleotide phosphate (NADH), and flavin adenine dinucleotide (FADH<sub>2</sub>). These four molecules are all produced in the mitochondria, but have a variety of purposes throughout the cell. ATP is the fundamental energy molecule that is used throughout most cell types of complex organisms. NADPH delivers energy for use in a variety of biosynthetic pathways. Lastly, NADH and FADH<sub>2</sub> carry energy during the production of ATP as well as being a source of energy in certain pathways (Wildman and Medeiros, 2015).

Out of the many molecules the body uses as energy molecules, the most significant is ATP. The goal of the reactions within the mitochondria is to produce this molecule. ATP is

composed of three phosphate groups bound to adenosine. However, when one of the bonds between the phosphates is broken it produces a large amount of energy as can be seen in *Figure 1.1*. Once this occurs the ATP molecule is converted to ADP (adenosine diphosphate) followed by AMP (adenosine monophosphate) through another bond breaking reaction. These molecules are typically in equilibrium with one another. For example, within a cell the ADP will bind pyrophosphate to form ATP to be used in a variety of other processes (Wildman and Medeiros, 2015). Throughout each cell the concentration of ATP is generally low but variable, rather than long term as it is constantly being used in a variety of processes.

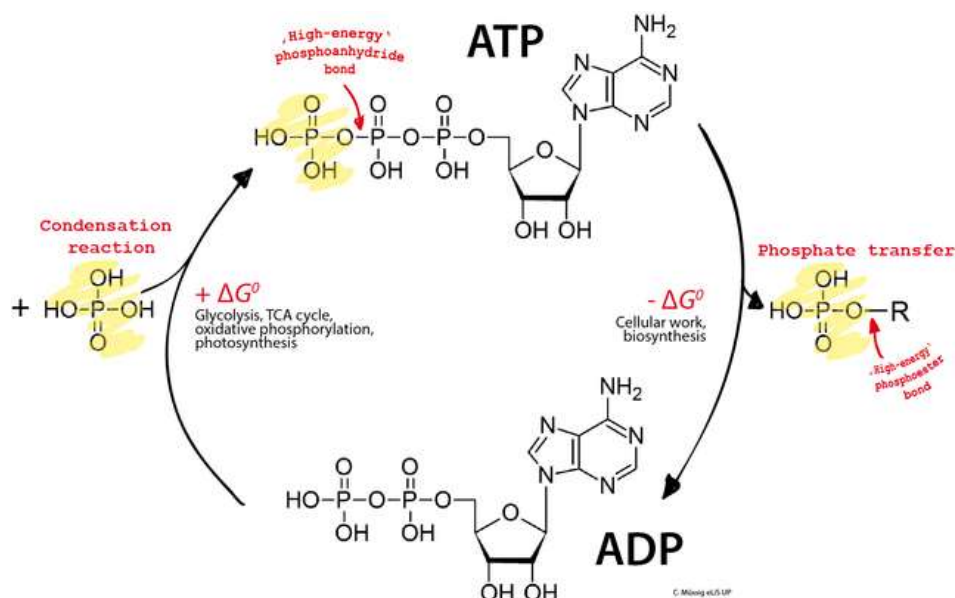


*Figure 1.1: An Equilibrium diagram of ATP conversion to ADP (Muessig, 2013). This depicts that when ATP is used it loses a phosphate group and is converted to ADP. This molecule will then be later condensed to ATP in a variety of reactions.*

NADH, FADH<sub>2</sub>, and NADH are used throughout the production of ATP in a variety of ways within the mitochondria, and are found in multiple other biosynthetic pathways as well. As nutrients are broken down, high energy electrons are released and need to travel from that location to the location of ATP production. These electrons travel from the site of nutrient breakdown to the site of ATP synthesis through the use of NADH and FADH<sub>2</sub>. NAD<sup>+</sup> is able to accept two high energy electrons and two hydrogen ions, forming NADH. Due to this ability, NADH is involved in several energy transfer reactions. FAD is converted into FADH<sub>2</sub> when it accepts two electrons and two protons. These two electron-accepting molecules are involved in a variety of similar reactions. NADPH is a molecule that has a similar purpose to the two previously mentioned molecules. This molecule in particular is an energy carrying molecule that

delivers energy to biosynthetic pathways. NADPH is structurally different from NADH because of an additional phosphate group, which causes these two molecules to have two different functions. NADPH drives biosynthetic processes and as this occurs it releases two highly charged electrons (Wildman and Medeiros, 2015).

### 1.1.2 The Electron Transport Chain

One of the most important aspects of cellular energy production is the electron transport chain, mainly due to the fact that this process is coupled with oxidative phosphorylation which is required to produce ATP. The electron transport chain is a series of redox reactions that occur as the electrons are passed between the four complexes (Karp, 2008). These reactions are coupled with the transfer of protons across the membrane to produce an electrochemical gradient. There are four membrane bound complexes named Complex I, Complex II, Complex III, and Complex IV that are responsible for the series of reactions involved in this process. All of these complexes are located on the inner mitochondrial membrane adjacent to the protein responsible for oxidative phosphorylation, ATP synthase (*Figure 1.2 below*) (Berg, 2002).

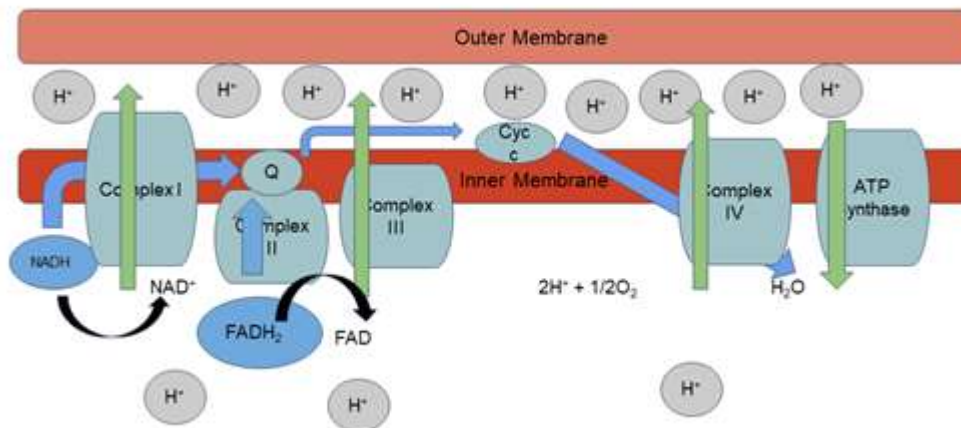


*Figure 1.2: A Diagram of the Electron Transport Chain coupled with Oxidative Phosphorylation. Protons are moved across a membrane as a variety of reactions occur. The proton then enter ATP synthase which uses them to convert ADP to ATP (Picture created by: Consedine, 2018).*

Three out of the four complexes (Complex I, Complex III, and Complex IV) involved in the electron transport chain are proton pumps and are solely responsible for pushing protons across the inner membrane in order to create an electrochemical gradient (Karp, 2008). Multi celled organism use oxidative phosphorylation to produce a large amount of energy is produced. However it is important to note that less complex organisms such as yeast can produce energy through fermentation. Each of the four complexes involved in the electron transport chain has a

specific, unique function that lead to the production of ATP through oxidative phosphorylation (Alberts et al., 2002).

Complex I contains a single molecule of flavin mononucleotide (FMN) which is also composed of eight or nine of iron clusters. The most common forms of these clusters is [2Fe-2S] and [4Fe-4S]. This particular complex has seven [4Fe-4S] and two [2Fe-2S]. The FMN is located at the end of a solvent exposed cavity, which is believed to form the NADH binding site. Some of the [4Fe-4S] clusters form a binding site for the coenzyme Q molecule (coQ) (Alberts et al., 2002). At Complex I two electrons are removed from NADH and transferred to coQ, thus producing QH<sub>2</sub> as a product. This product (QH<sub>2</sub>) is allowed to freely diffuse across the inner membrane and transfer four protons to the intermembrane space, which begins the formation of the proton gradient. This “proton pumping” mechanism is driven by a conformational change in Complex I, which is the result of the change in the redox state of the protein (Voet, Voet & Pratt, 2012). This complex is the site of a sizeable amount of electron leakage due to the high attraction between free electrons and oxygen.

Complex II is commonly known as succinate-coenzyme Q oxidoreductase and contains four subunits. This complex participates in both the electron transport chain and the citric acid cycle. Complex II contains a covalently bonded FAD molecule, one [4Fe-4S], one [3Fe-4S], one [2Fe-2S], and one cytochrome molecule (Voet, Voet, & Pratt, 2012). At this complex, succinate (which is a product of the citric acid cycle) transfers electrons to coQ. The free energy created from this reaction is unable to drive ATP synthesis on its own. Unlike Complex I, no protons are transferred into the intermembrane space as a result of the electron transfer, thus, this complex overall transfers less energy (Berg, 2002).

Complex III, also known as coenzyme Q-cytochrome c oxidoreductase, contains the following molecules: two b-type cytochromes, one cytochrome c, and one [2Fe-2S] cluster. Complex III, in particular, contributes to the asymmetric absorption and release of protons. The reactions at this complex is a two-step process that allows one molecules of QH<sub>2</sub> to transfer its electrons to cytochrome c (Berg, 2002). The first reaction permits QH<sub>2</sub> to bind and transfer one of its electrons to the iron cluster, releasing two protons. Due to this first reaction set, the [2Fe-2S] iron cluster then reduces one molecule of cytochrome c. The newly formed coQ molecules then rebinds to complex III, where it gains another electron to return to a partially reduced state (Voet, Voet, & Pratt, 2012). The second reaction set follows a similar manner of reactions,

however at the end of this reaction a fully reduced coQ molecule is formed and four protons are moved across the membrane.

Cytochrome c oxidase, or Complex IV, contains two different cytochrome molecules and two different copper atoms. At this complex, two simultaneous reactions occur that affect the overall transmembrane proton gradient. As this complex reduces molecular oxygen and produces two water molecules, four protons are taken up by the complex (Voet, Voet, & Pratt, 2012). Thus, the proton concentration in the matrix is lowered significantly. As this reaction occurs these four protons are “pumped” across the membrane in each reaction step. Eight positive charges are lost from the matrix to the intermembrane space and contribute to the membrane potential difference that drive ATP synthesis (Karp, 2008). Unlike the three other complexes, the exact mechanism of action for complex IV is still largely unknown.

As mentioned previously, the electron transport chain is coupled with a process called oxidative phosphorylation. During this process ATP is produced through the use of the electrochemical gradient created during the electron transport chain and the utilization of the  $F_0F_1$  ATP synthase (Senior, Nadanacvia, & Weber, 2002). As can be seen in *Figure 1.3*, the protein complex is composed of several different sections that all have specialized purposes. The  $F_0$  protein is composed of three subunits called subunits a, b, and c and act as an ion channel (Jonckheere, Smeitink, & Rodenburg, 2012). The number of c subunits determines the number of protons that are needed to make the  $F_0$  turn a full revolution. The number of c subunits is species dependent; in humans eight protons are needed, *C. elegans* require one proton, and mice need four protons.

In the c subunit, aspartic acid and glutamic acid are present while the a subunit contains an arginine residue. All of these residues are highly conserved among species, and believed to

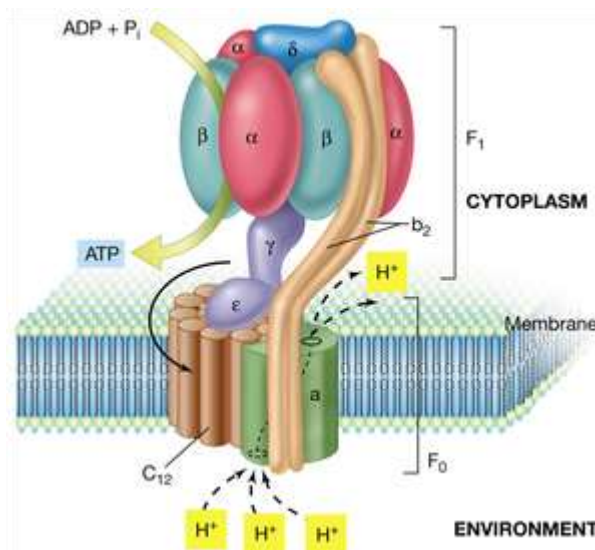


*Figure 1.3: A Structural Diagram of the ATP Synthase Protein Complex. Protons are moved into subunit a which causes subunit c to move which allows for the  $F_1$  complex to rotate and ATP to be produced. (WordPress, 2015)*

play an important role in proton translocation (Yasuda et al., 1998). The most widely accepted model for proton translocation is the “two channel model”. In this model, it is assumed that the a subunit has two channels that run half the membrane but on different sides. These channels connect the proton binding site with the cytoplasm and each channel is in contact with a different c subunit. The proposed mechanism follows this pathway: a proton enters from the cytoplasm side and binds to the carboxyl residue in the c subunit (Okuno, Noji, & Lino, 2011). This offsets the negative charge on the carboxyl group which allows the c subunit to rotate apart from the a subunit toward the lipid bilayer. As this happens, the c subunit at the lipid bilayer makes contact with the other half channel. This promotes the deprotonation of the carboxyl residue and the proton enters the cytoplasm.

Once the c subunit is filled, it produces free energy, driving the  $F_1$  component of ATP synthase and beginning ATP production. The  $F_1$  component of ATP synthase is composed of  $\alpha$ , B,  $\gamma$ , and  $\epsilon$  subunits. The  $\alpha$  and B subunits form a hexamer (Senior, Nadanacvia, & Weber, 2002). The other subunits involved in this mechanism are part of the rotational component of ATP synthase. Subunit B is where ATP is produced and goes through a series of conformational changes called the loose state, the tight state, and the open state (Jonckheere, Smeitink, & Rodenburg, 2012). Each catalytic site goes through each transition state during a  $360^\circ$  rotation as can be seen in *Figure 1.4*. The mechanism starts by binding adenosine diphosphate (ADP) and inorganic phosphate ( $P_i$ ) to the open state. This subunit then goes into the loose state upon binding these molecules. During this same step, the ATP leaves the complex as the conformational change occurs and it is now in the open state. ADP and  $P_i$  now bind to the newly empty open state while the ADP and  $P_i$  in the tight are converted into ATP (Nakamoto, Baylis, & Al-Shawi, 2008). The process then repeats where the ATP in the tight state leaves as it is now in the open state and the whole process begins again. At the end of each rotation three ATP molecules are produced as a form of energy for the organism, indicating that each  $120^\circ$  rotation produces 1 molecule of ATP.

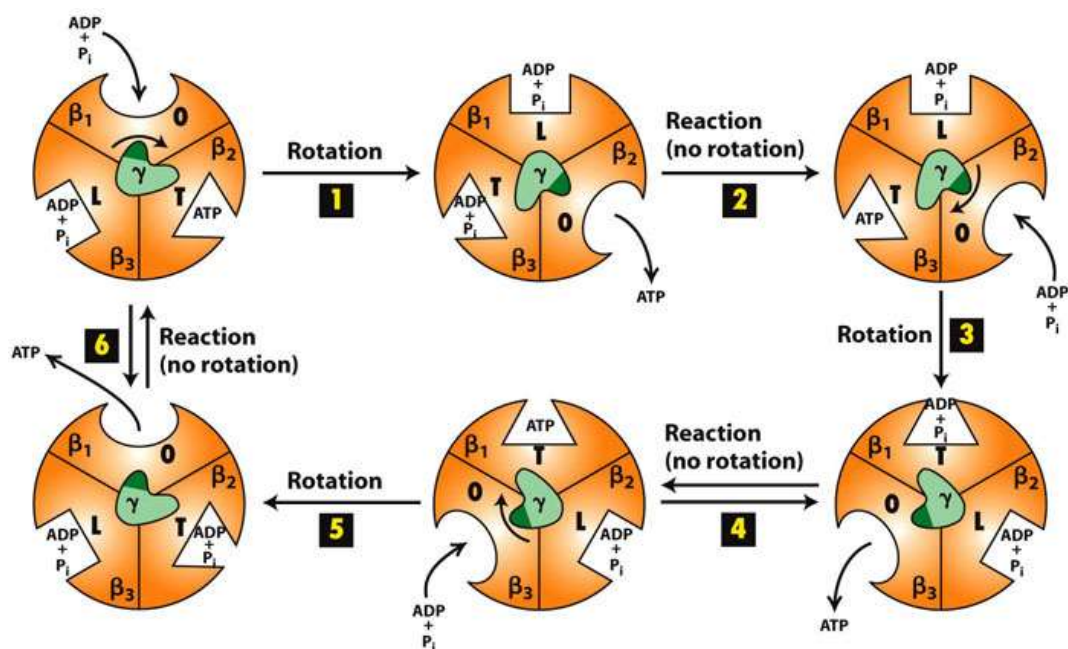


Figure 1.4: A Rotational Diagram of the F<sub>1</sub> Subunit in ATP Synthase. ATP and a phosphate group enter when one part of the  $\beta$  subunit is open which causes it to convert to the loose state. Once another ADP and phosphate group binds, the structure rotates and the first  $\beta$  subunit changes to the tight and converts ADP to ATP. the  $\beta$  subunit then rotates which releases the newly made ATP molecule as the  $\beta$  subunit is again in the open state.

(University of Miami, n.d.)

## 1.2: Metabolism and Neurodegeneration in Humans

### 1.2.1 Overview of Metabolic Disorders

Metabolic diseases alter normal processes which result in biochemical abnormalities from a shortage of a particular enzyme or malfunctioning organelle. Most metabolic disorders are inherited in an autosomal recessive pattern, but some have been observed to be inherited in x-linked or autosomal dominant manners. These disorders are further classified into three different categories. The first class is composed of disorders defined as the buildup of toxic compounds in the organism. The second class are disorders due to low amounts of energy. The third are disorders involving complex molecules not involved in the diet. These disorders occur in one in every five thousand live births and are considered fairly rare. Generally, metabolic disorders have nonspecific symptoms, which means there are no strict set of symptoms that indicate someone might have one. The symptoms of metabolic disorders vary from one another since they affect different processes in different areas of the organism (Graef, Wolfsdorf, & Greenes, 2008). Two examples of this are Diabete Mellitus (DM) and Wilson's Diseases.

DM is a group of metabolic disorders that occurs when the body fails to produce or use insulin effectively. There are two types of this disease known as type 1 diabetes or type 2 diabetes. These two variations of the disease have different causes but result in similar symptoms (Brutsaert, 2017). Approximately 347 million people currently live with diabetes mellitus worldwide. Type I DM is characterized by the lack of insulin production in the body. The cause of type I DM is the autoimmune destruction of pancreatic beta cells. These cells are destroyed over months to years and continue until the concentration of glucose in the body can no longer be controlled. This type of DM typically occurs in children but can manifest in adults in rare cases. (Brutsaert, 2017). Type II DM is characterized by the inability to use insulin properly in the body. In this case, the patients have become resistant to insulin and cannot uptake glucose as a result. 90% of cases of DM worldwide are type II. The cause of this form of DM is related to lack of physical activity and excess body weight. The symptoms for type II DM are extremely similar to type I, however unlike type I, type II can occur in both adults and children. If caught early enough it is completely treatable with the proper medication, but can go unnoticed for years (Brutsaert, 2017).

Wilson's Disease is another metabolic disorder that is considered rare as it causes the accumulation of copper in vital organs such as the liver or the brain. This disease is an autosomal recessive disorder that causes a mutation in the ATP7B gene and it occurs in approximately one in every thirty thousand people. People are typically diagnosed with Wilson's Disease between the ages of 5 and 35 (Mayo Clinic, n.d.). This disease is technically present at birth but symptoms do not begin to manifest until the copper accumulation builds up to significant levels. The symptoms of this disease vary depending on the location and severity of copper build up (NDDKD, n.d.). Due to the fact that this disease is a genetic disorder, treatment will be a lifelong regimen for those that have this disease. Treatment is a two-step process for those that have Wilson's disease. The first is a chelating agents, which bind copper and then causes the organs to release all the copper in one's body which is then filtered out of by the kidneys. The second step is taking medication that prevents the buildup of copper from occurring again. With these palliative measures this disease is manageable but a lifelong fight for those who live with it (Mayo Clinic, n.d.).

### 1.2.2 Neurodegenerative Diseases and Metabolism

Many diseases that are associated with aging exhibit symptoms that are representative of functional loss of nervous and muscular systems, both of which are regulated by metabolism. Many patients diagnosed with classical neurological disorders, including Amyotrophic Lateral Sclerosis, Huntington's Disease, and Parkinson's Disease also exhibit symptoms that directly indicate loss of function of key regulatory pathways. This is indicated in symptoms including unexplained weight loss, unsteady glucose levels, and lethargy.

Neurodegenerative disease can present themselves in many different ways. Amyotrophic Lateral Sclerosis is classified by the impairment and cell death of motor neurons. Degeneration of the motor neurons begins in the cortical nervous system, brainstem and spinal cord. Patients with ALS are often found to go into acidosis, which breaks down the lipids in the body (Dodge et al., 2013). Parkinson's Disease also affects motor neurons. Mutations in a series of PARK genes cause the buildup of a misfolded protein,  $\alpha$ -synuclein that is found at neuronal synapses. This causes the neurons responsible in dopamine production to die. Maps of the brains of Parkinson's patients have been created, and it has been found that glucose is metabolized more slowly by those affected (Anadahan et al, 2017). Altered metabolism in brains of Parkinson's patients can be seen in *Figure 1.5*. Huntington's progressively wipes out both motor and cognitive abilities in patients. A mutation in the HTT gene codes for Huntington's protein. Huntington's proteins lengthens polyglutamate tract with an exon of a repeating CAG mutation. One of the key causes of cognitive degeneration in Huntington's Disease is the impairment of over 60 metabolites in the brain (Patasini et al, 2016).

Amyotrophic Lateral Sclerosis, Parkinson's Disease, and Huntington's Disease are all considered classical neurological disorders as the classifying symptoms relate the brain and overall degradation of the nervous system. The mechanisms of neurodegeneration vary between diseases, but all result in some form of dementia. Presentation and severity of dementia can vary

between diseases, but the main characterization is the loss of memory and learned everyday skills.

Neurodegeneration is a high rate of neuronal cell death (Saba, 2015).

The increased death of neuronal cells can be directly linked to disruptions in the organism's biological function, specifically in the electron transport chain and energy levels. All cells need energy in order to survive. As the mitochondria fail, an overload of oxidation breaks down the proper transfer energy. When this disruption occurs in the mitochondria of neuronal cells, the nervous systems begins to deteriorate at a rapid rate. Neurons, unlike other adult cells, do not undergo replication. If a neuron dies, it is not replaced, allowing mitochondrial dysregulation to quickly become a problem. Anatomically, Amyotrophic Lateral Sclerosis, Parkinson's Disease, and Huntington's Disease affect the hypothalamus in the brain. This region plays a key role in metabolic functions, as it controls energy transport throughout the body (Saba, 2015).

Currently, doctors do not have any cures for these neurodegenerative disorders. The only treatments available are those to relieve symptoms and make patients more comfortable. Generally, these medications are only able to target one symptom at a time, making patients take a cocktail of various treatments. If doctors are able to find the origin of neuronal cell death, they may be able to stop these catastrophic effects (Cai et al, 2012).

### 1.2.3 Metabolism in classic Neurodegenerative Disorders: Alzheimer's Disease

Alzheimer's Disease is a classical neurodegenerative disorder, characterized by the degradation of cognitive function and the onset of dementia. In the United States, Alzheimer's

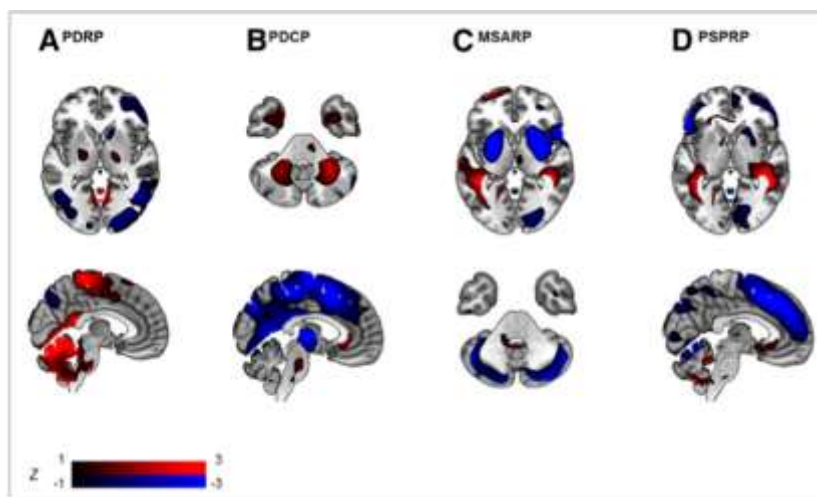


*Figure 1.5 Metabolic activity in brains of Neurodegenerative Diseases. Cross section A is showing the Parkinson's Disease related patterns (PDRP), B is the Parkinson's Disease Cognition Pattern (PDCCP), C is the Multiple Systems Atrophy Related Patterns (MSARP), and D is Progressive Supranuclear Palsy related pattern. Red is indicative of increased metabolism and blue is indicative of decreased. This figure was originally published in Meles et al., 2016.*

Disease is the leading cause of dementia and the 6th leading cause of death. *Figure 1.6* shows how the condition is spreading across the nation. People can develop Alzheimer's disease one of two ways. Most people develop Alzheimer's sporadically, however, a small part of the population inherit Alzheimer's disease. The inherited form of Alzheimer's disease is classified as early onset, as most patients develop symptoms before age 65 (Cai et al, 2012). Several genes have been linked to Alzheimer's Disease, but one of the main questions that researchers still struggle to understand is how these genes are mutated in the first place (Grant et al., 2013).

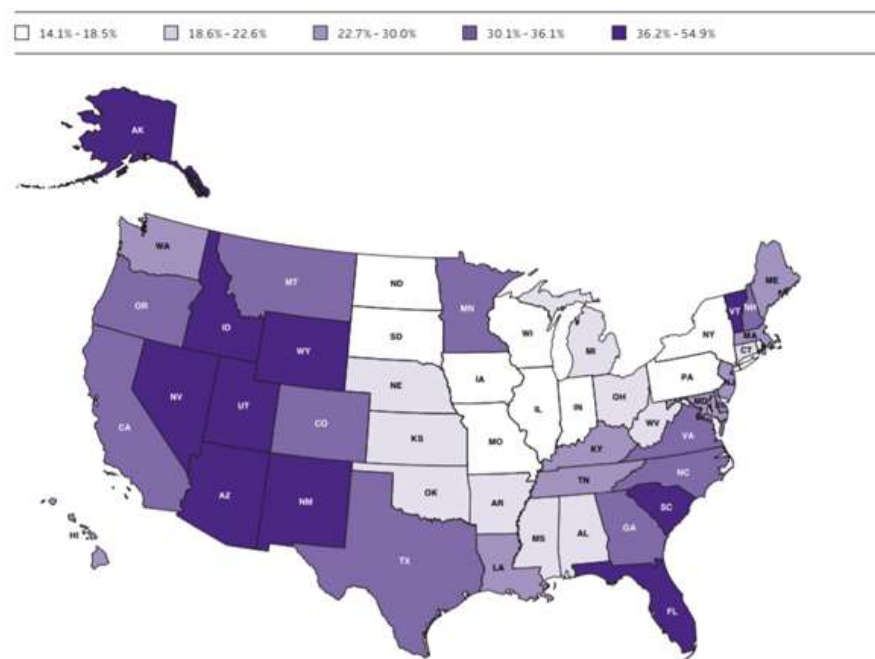


*Figure 1.6* Map of the United States showing the increase of Alzheimer's Disease by state as projected to 2025. The darker the shade of purple, the higher the growth rate. This image was originally published on the Alzheimer's Association web page (2017).

Alzheimer's disease is characterized by extraneuronal amyloid- $\beta$  plaque accumulation in the brain and neurofibrillary tangles. Amyloid- $\beta$  peptide ( $A\beta$ ) is derived from the amyloid precursor protein (APP), which is processed by  $\beta$ -secretase and  $\gamma$ -secretase.  $\beta$ -secretase cleaves APP into  $sAPP\beta$ , and  $\gamma$ -secretase cleaves the cytosolic portion of the protein, releasing amyloid- $\beta$ . The accumulation of this protein is associated with the progression of neurodegeneration and the symptoms of Alzheimer's Disease (Price, Morris 1999). In addition to neurodegeneration, amyloid- $\beta$  plaques also accumulate in the mitochondrial matrix of cells causing problems in energy processing. Most notably is the enzyme alterations occurring at multiple steps in the

Kreb's Cycle that can be identified in those suffering from AD. Improper glucose processing toxifies the mitochondria with unhealthy levels of byproduct intermediates (Chen & Yan, 2006).

Both early onset and non-inherited Alzheimer's Disease are classified by neurological lesions produced through an inherited or developed genetic mutation. The lesions are the Beta amyloid plaques and neurofibrillary tangles. Plaques are built up of the beta amyloid proteins, and neurofibrillary tangles are built up of the microtubule Tau proteins. Both aggregate in the brain and disrupt neurological functions, eventually leading to cell death (Cai et al, 2012). *Figure 1.7* illustrates the accumulation of these proteins in neurons.

A physical symptom of Alzheimer's Disease is the degradation of the olfactory system resulting in the loss of smell, also known as anosmia. It is believed that the loss of smell is occurring in not the peripheral but the central nervous system, as the smells are sending signals to the brain but the signals are not being processed correctly (Hawkes, 2003). One of the main concerns with measuring anosmia in Alzheimer's patients is ensuring the loss is an olfactory defect as opposed to a cognitive defect. To address these concerns, studies on olfaction have been conducted on patients whose memory and mini-mental state examination (MMSE) scores show only mild cognitive impairment. These patients were still able to perform normally on verbal/visual matching tests. These studies have allowed researchers to determine that the anosmia exhibited by those affected by Alzheimer's Disease is more strongly linked to olfactory dysregulation, rather than cognitive ability. The presentation of olfactory defects in those with mild cognitive impairment validates anosmia as an early quasi-diagnostic symptom of Alzheimer's (Luzzi et al., 2006).

The mitochondria have been identified as a key organelle for research. Mitochondria have sparked such interest due to their degradation with age, and ability to disrupt protein formation and oxidative phosphorylation when not functioning properly (Grant et al, 2013). This has caused researchers to propose a new model for Alzheimer's disease. In this new model, Alzheimer's patients have a decreased energy flow from both

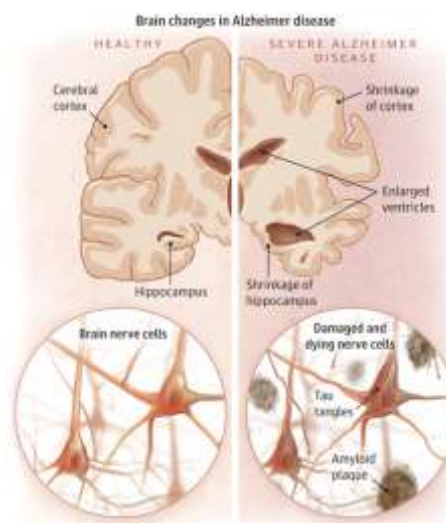


*Figure 1.7: Neurological lesions found in brains of Alzheimer's Disease patients.*

(Jin, 2015)

glycolysis and oxidative phosphorylation, resulting in increased lactate. When the mitochondria detect this decrease of energy flow, they upregulate the oxidative phosphorylation. When this increases, it also increases the amount of reactive oxygen in the system. Reactive oxygen are free radicals, and they cause oxidative stress. Oxidative stress damages cells, causing DNA damage and eventual cell death. If this is happening in the brain, it leads to neurodegeneration (Demetrius, Driver, 2013).

#### 1.2.4 Polyphenols in Therapeutics

All plant matter contains a group of compounds called phytochemicals, and are responsible for protecting against certain diseases. A type of phytochemical is polyphenols. These compounds have a variety of structures but contain one or more phenolic ring. Two examples can be seen below in *Figure 1.8*. Polyphenols can be classified into several different categories phenolic acids, flavonoids, phenolic alcohols, stilbenes, and lignans. Polyphenols also have “pro-oxidant properties”, which work against their natural metabolic activity (Abbas et al., 2017). Due to this property, it has the possibility to block cell propagation and apoptosis as well as reduce telomerase and lipoxygenase activity.

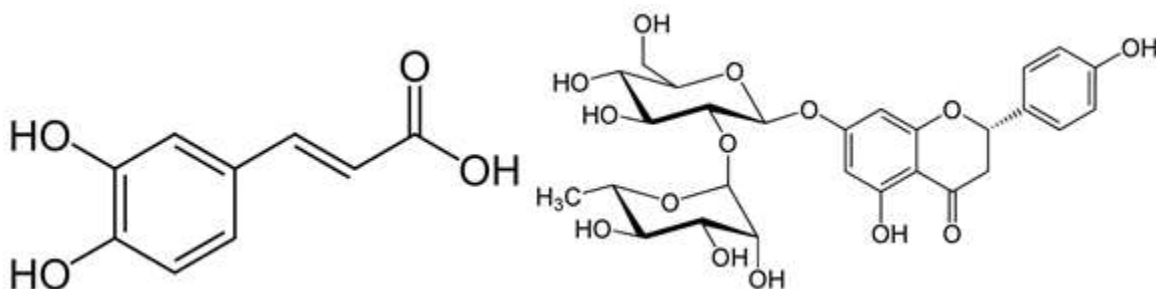


*Figure 1.8: Two Examples of different polyphenols. The left shows the compound caffeic acid, a polyphenol naturally found in various plant species such as mushrooms, freshwater ferns, and the bark of the Southern Bluegum tree. The structure on the right is naringin. It is found in various citrus based fruits, specifically grape fruits.*

To express their biological properties, polyphenols depends heavily on their bioavailability. Their structure also determines how fast they are absorbed and the limit of absorption in the intestines. Typically polyphenols have one sugar substituent but can have up to three, with a wide range of sugars that can be added. Glycosylation, the attachment of sugar groups to other functional groups, determines the physical, biological, and chemical properties that each polyphenol exhibits. These molecules undergo reactions as they travel throughout an organism, specifically in the human small intestine (Abbas et al., 2017). The first reaction occurs

as the molecules travel in the small intestine. The polyphenols are digested by various enzymes into their more bioavailable metabolite. As they travel, they simultaneously inhibit pathogenic microbe growth and promote the growth of beneficial bacteria in the gut microbiome (Manach et al., 2004). Both of these result in an overall healthier organism as the more beneficial bacteria are more prevalent and the polyphenols are more available for use.

As such, polyphenols can be used as therapeutic compounds for a variety of diseases and illnesses. These disease include, but are not limited to: cardiovascular disease, cancer, osteoporosis, neurodegenerative diseases, and diabetes mellitus (Manach et al., 2004). In terms of cardiovascular disease, it has been shown that the consumption of polyphenols reduces the risk of a cardiac episode. However, there is currently no one polyphenol isolated as a treatment, because they all reduce blood pressure, improve the functional capabilities of epithelial tissue, and inhibit platelet aggregation by the reduction of lipoprotein. The mechanism of action for polyphenols in cardiovascular health has been determined to modulate the activity of nitric oxide synthase and its bioavailability, which has an important role in myocardial tissue (Abbas et al., 2017).

Through different studies, it has been shown that polyphenols alleviate the side effects of type two diabetes in several different ways. One mechanism that has been observed is through the inhibition of disaccharides in the intestinal lumen (Anhê et al., 2013). This limits the digestion of polysaccharides and the absorption of simple sugars by the body. One of the major characteristics of type two diabetes is the hyperglycemic condition caused by an increase in glucose production and lack of glucose storage. Through the use of polyphenols, glucokinase activity increases, increasing glucose storage and decreasing production. Additionally, polyphenols have been shown to protect  $\beta$ -islet cells from glucotoxicity, a common side effect of hyperglycemia. Generally, polyphenols increase insulin production of the  $\beta$ -islet cells and help to stabilize blood glucose levels (Anhê et al., 2013).

When it comes to the brain, studies have shown that both lifestyle and genetic factors the development of neurodegenerative diseases and overall cognitive function as age progresses. Studies have indicated that those with a high polyphenol diet reduces the risk of dementia and improved cognitive function. Specifically catechins, theaflavins, flavonols, and hydroxybenzotic acids all have a positive effect on verbal memory and language (Vauzour, 2012).

In neurodegenerative diseases such as Alzheimer's Disease, polyphenols exhibit neuroprotective properties. In one study that utilized a mouse AD model, resveratrol, a polyphenol found in grapes was shown to increase their cognitive function (Bhullar & Rupasinghe, 2013). This compound prevented A $\beta$  formation and protected neurons from A $\beta$  toxicity by impeding the enzyme nitric oxide synthase. In a transgenic mouse model, grape extracts prevented A $\beta$  oligomerization on a cellular level and generated an increase in cognitive function in those mice on a behavioral level. Another study, indicated that the same grape extracts prevented the abnormal folding in tau proteins in AD. Another research team showed that the metabolite epigallocatechin gallate increased synaptic transmission in the binding protein associated with cyclic adenosine monophosphate (cAMP) (Bhullar & Rupasinghe, 2013). Other neurodegenerative disorders such as Huntington's Disease and Parkinson's Disease have also shown to have reduced symptoms when treated with polyphenols. This trend between polyphenols and the improvement of patients with neurodegenerative disorders indicates a potential new family of therapeutic measures for these diseases.

### **1.3 C. *elegans* as a Model Organism**

#### **1.3.1 The Life Cycle of *C. elegans***

The study of human biology through the use of model organisms has allowed for significant advances in the field of biology. Observation, characterization, and manipulation of specific biological processes in non-human organisms have opened windows into the inner workings of homologous processes in humans.

*Caenorhabditis elegans* (*C. elegans*) is a useful model organism for many reasons, the most significant of which is its organismal simplicity. These roundworms belong to the Chromadorea class of nematodes, are non-parasitic, and measure about 1 mm in length as adults. Wild-type *C. elegans* populations contain mostly hermaphrodites and a miniscule frequency of males (one male to every 1,000 hermaphrodites), allowing for self-fertilization and simple maintenance of large and genetically homogenous populations. Hermaphrodites carry five autosomes and two X chromosomes, while males have the same five autosomes but only one X chromosome. The worms themselves are eutelic and anatomically simple. They exhibit a tapered outer body tube containing the worm's dermis, muscular and nervous tissue, and excretory organs, and an inner tube containing the worm's reproductive organs and intestinal tract (Mango, 2007). The nervous system contains around 300 neurons yet is fairly sophisticated, with both

central and peripheral divisions. This grants the worms with the capability of active decision making, voluntary motor functions, and neural plasticity (Mango, 2007).

The life cycle of *C. elegans* is divided into 4 larval stages (L1-L4), two adult stages (young adult and adult), and two conditional starvation stage (pre-dauer and dauer). Worms with adequate amounts of food on their plates progress from the L1 stage to adults in 3.5 days when grown at 20°C. Once a hermaphroditic worm reaches adulthood it begins to fertilize oocytes and can lay eggs for up to three days, with potentially hundreds of progeny. Under starvation conditions, freshly hatched worms enter the L1 arrest stage, which increases the larva's resistance to environmental stressors and stops development (Baugh, 2013). In this state, the worm can survive for several weeks without food. Once food is introduced back into the environment, the worm exits L1 arrest and returns to the first larval phase (L1) to continue development (as seen in *Figure 1.9*). Dauer formation, however, is more complex--it is induced by pheromone signaling from other worms in the vicinity, generally as a result of overcrowding, starvation, or high temperature. Unlike L1 arrest, the Dauer stage is associated with a morphologic change in the worm's structure. The worm shrinks in size and feeding behaviors and general mobility are greatly suppressed. In this stage, the worm can survive up to 4 months without food, and will exit Dauer stage directly to L4 upon encountering a more favorable environment with more alimentary resources (Baugh, 2013).

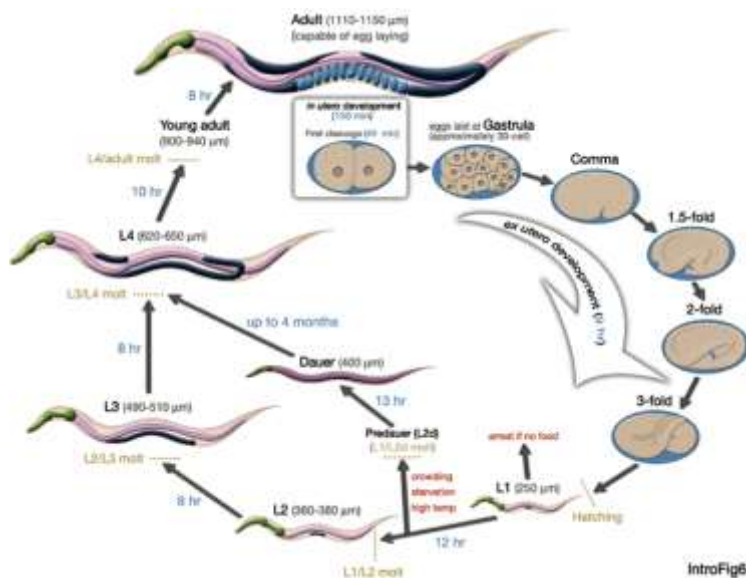


Figure 1.9: *C. elegans* life cycle (Wormbook, 2018)

Hundreds of worms can be cultured on a single NGM plate seeded with uracil-dependent *Escherichia Coli* OP50, and can be grown at different temperatures to vary both the speed of life

cycle and the population fraction of males. While worms are easy to culture and maintain, extended storage is also possible through live culture freezing. Original stock worms are preserved in M9 and glycerol and are frozen using liquid nitrogen in order to avoid genetic drift in extended subcultures in lab (Brenner, 1974). In addition to ease of culture, there is also a substantial foundation of research that enables researchers to investigate and manipulate specific metabolic processes and genetic loci. *C. elegans*' entire genome was sequenced in 1998, and 60-80% of the encoded genes are homologous to human genes. In addition to this, 40% of human genetic diseases have homologous genetic mutations in *C. elegans* that can simulate analogous disease states (Kaletta and Hengartner, 2006). Naturally induced mutations, transgenic mutations, and RNAi are all tools that can be used to simulate disease states or conditions, and can easily be maintained in hermaphroditic worms.

### **1.3.2 *C. elegans* as a model for metabolic disorders**

The simplicity of *C. elegans* makes it a great platform to model human diseases because of the many homologous structures and pathways it shares with humans. Specifically, *C. elegans* can be used as a model for metabolic disorders and imbalances. The wealth of available research on *C. elegans* has allowed scientist to establish comprehensive metabolic network models of wild-type metabolism. These models also predict behaviors and outcomes in altered metabolic states. Many metabolic pathways and processes in worms are homologous to human pathways, such as the electron transport chain, and allows for targeted interventions in *C. elegans*. Since structure and function of each of the mitochondrial complexes are generally highly conserved between species, they serve as a good predictor of human mitochondrial function (Moreno-Arriola et al. 2014)

Additionally, *C. elegans* has been used extensively as a model for oxidative stress and related diseases. Modification of the production of radical oxygen species and biological systems for oxidative protection allows for deeper investigation into the metabolic mechanisms of stress in disease states. One such disease is diabetes mellitus, whose exact mechanisms of pathogenicity are not yet fully understood, but exhibits increased mitochondrial production of superoxide ( $O_2^{\bullet-}$ ) (Moreno-Arriola et al. 2014). Worms have similar reactions to oxidative stress on a cellular level, and also exhibit the same overproduction of radical oxygen species when exposed to glucose. Along with these similarities, *C. elegans* also contains an insulin-like signaling pathway that is involved in the regulation of longevity, metabolism, and growth (Lee et

al. 2001). Modeled insulin-deficient worms have been created to study diabetes mellitus that exhibit distinct behavioral phenotypic deficits not unlike human diabetic patients. Defective insulin production or interruption of the insulin-related growth factor 1 (IGF-1) pathway analog DAF-2 results in slowed growth, increased general longevity, and increased longevity of each growth stage (Fuchs et al., 2010). Changes in longevity are a common phenotype exhibited in metabolic mutants, but are generally difficult to assay in a laboratory setting. Well-established behavior patterns in *C. elegans* serve as excellent baselines to which metabolic mutant activity can be compared.

### 1.3.3 *C. elegans* as a model for AD

One of the most apparent parallels between *C. elegans* and humans is the nervous system, which allows for simulation of neurological disorders. One such disorder that can be modeled is Alzheimer's disease (AD). *C. elegans* express an analogous pathway that cleaves APL-1 instead of A $\beta$ . APL-1 and A $\beta$  are similar in both function and sequence, with similarly conserved cytosolic, E1, and E2 domains. APL-1, however, doesn't contain the necessary A $\beta$  domain characteristic of the amyloid- $\beta$  plaques (Alexander et al., 2014). In order to more accurately model AD, a transgenic strain was created that encodes the human A $\beta$ <sub>1-45</sub>, the peptide found in amyloid plaques. The first to employ this pathway in *C. elegans* was Chris Link, who created the first AD transgenic *C. elegans* in order to assess treatment efficacy outside of mammalian subjects (Dostal and Link, 2010).

Transgenic worms that express A $\beta$  in muscular and neuronal tissues do not survive past the first larval stage, but specific expression of A $\beta$  in either neuronal or muscular tissue results in a viable worm model of AD with cognitive and locomotive impairments, respectively. Both the muscular and the neuronal models' transgenes are expressed at temperatures exceeding 20°C, so worms are maintained at 16°C and are heat-shocked at 25°C for expression of A $\beta$  (Dostal and Link, 2010). Although typical symptoms of cognitive impairment (such as memory loss) of AD cannot be measured in *C. elegans*, general nervous system integrity and cognitive ability can be assessed in a laboratory setting. The worm's chemosensation relies on amphid sensory cilia and sensory neurons to interpret chemical signals and relay them to the worm's central nervous system. Olfactory impairment is a key symptom in AD; many patients present with anosmia in early stages of the disease (Olichney et al., 2005). In this way, sensory assays evaluating

olfaction in *C. elegans* serve as a good measure of disease morbidity and allow for the evaluation of potential treatments.

#### **1.4 New Directions: Our Project Overview**

Previous projects have been able to classify phenotypes in the transgenic worms expressing various neurodegenerative disorders through behavioral assays. These phenotypes are due to under and over expression of various proteins in the system associated with the individual disorders. This project continued forward with treating transgenic Alzheimer's Disease worms with punicalagin, however, the goal of the project was to link Alzheimer's Disease with an electron transport chain defect. To link Alzheimer's Disease with the electron transport chain, worms mutated to have deficient electron transport chains were also tested.

In order to link Alzheimer's Disease with defects in the electron transport chain, all of the worms needed to be tested under two different treatment conditions, punicalagin and coenzyme Q<sub>10</sub>. Wild-type, transgenic Alzheimer's, and metabolic mutant worm strains were given OP50, OP50 with punicalagin, and OP50 with Coenzyme Q<sub>10</sub>, and examined with three behavioral assays: avoidance, chemotaxis, and locomotion. These behavioral assays provided information in order to describe phenotypes of each worm depending on their overexpression of the beta amyloid plaques in the nervous system, or under expression of coenzyme in the electron transport chain. Following, the worms under each treatment were also tested to determine ATP levels via a bioluminescence assay. This allowed the overall energy in the worms to be monitored before and after exposure to the various treatments in order to determine if a connection is present between Alzheimer's Disease and an under functional electron transport chain.

## 2. Methodology

### 2.1 Worm Protocol

#### 2.1.1 Maintenance

*C. elegans* are maintained on Nematode Growth Medium agar (NGM) in 60 mm plates, which allow for growth of large populations sufficient for multiple assays. Each NGM plate was seeded with several drops of LB broth inoculated with OP50 *E. coli*, and were left to dry for approximately 24 hours before being used. Once dry, several adult worms from a single strain were passed from a parent plate to a new daughter plate using a titanium wire pick. Before picking, the wire was sterilized by passing through an open flame. Worms were also moved through “chunking”, a method that utilizes a metal spatula (dipped in ethanol and flamed) to slice out a small square of agar and transfer the square face down to the daughter plate. Passed plates were labeled with the passer’s initials, worm strain, treatment, and the date passed.

Once passed, plates were observed frequently in order to maintain a healthy worm line. *C. elegans* growth rates are highly dependent on culture temperature, overcrowding and amount of food. If a plate is left to culture for too long, the lack of food will drive worms into the dauer stage, leaving no viable adults for testing purposes. In order to ensure a healthy adult population, worms were picked every 1-3 generations. If plate contamination became an issue, a few different methods can be used to eliminate it, depending on the severity. In the case of mild contamination, worms were picked to a seeded plate for one to two days, then after this period of time the same worms were then transferred to another seeded plate for culture. If contamination was more severe, worm bleaching methods were used. Three gravid adult worms were picked from the contaminated plate and placed in a 20 $\mu$ L drop of worm bleaching solution on a fresh seeded plate. The solution kills the worms but leaves the eggs intact, which develop once several days pass and the bleach evaporates (Stiernagle, 2006).

#### 2.1.2 Strains

The N2 strain of *C. elegans* are a wild-type strain discovered in the 1940s, but were first investigated and described by Sydney Brenner in his groundbreaking paper, “The Genetics of *Caenorhabditis Elegans*” in 1973. These worms were gathered from a compost pile in Bristol, England in the 1950’s, and serve as a baseline for assays and treatment effects. Worms develop fully in 72 hours, and gravid worms can lay upwards of 300 eggs in a lifetime (source).

CL4176 and CL2355 are Alzheimer's Disease-modeling transgenic strains that produce human beta amyloid peptide, one of the main hallmarks for AD. They were chosen because they are the closest pathological analog of AD in *C. elegans* and exhibit similar phenotypic characteristics of the disease. Full expression of A $\beta$  in neuronal and muscular worm tissues causes the line to be non-viable, so two strains were created: CL4176 (*smg-1(cc546) I; dvIs 27 [myo-3p::A-Beta (1-42)::let-851 3'UTR) + rol-6(su1006)]*), with AD gene expression only in the muscular tissue, and CL2355 (*dvIs [pCL45 (snb-1::Abeta 1-42)::3' UTR(long) + mtl-2::GFP]*), with expression in only neuronal tissue. CL2355 exhibit neuronal deficits, which can be observed in chemotaxis and avoidance scenarios, but otherwise develop normally. CL4176 exhibits muscular impairment at all temperatures; the worms are unable to travel in the normal sinusoidal pattern and instead turn in a small circle, with limited control over muscular contraction. CL4176 worms are also maintained at 16°C, as higher temperatures modulate gene expression--for full expression of A $\beta$ , worms are heat shocked at 25°C. These strains were created by Christopher Link at the University Colorado, Boulder in order to study the effects of A $\beta$  in living organisms in a high-throughput testing fashion. (Lublin & Link, 2013).

*Clk-1* (*clk-1(e2519) III*) is the first of the two metabolic mutant strains tested in this project. This strain contains a mutation in the *Coq7/Cat5* gene (a human *Coq-7* homolog) that encodes DMQ hydroxylase, an enzyme necessary for the synthesis of ubiquinone (*clk-1* (gene).2007). Ubiquinone, or coenzyme Q, is a critical component in the mitochondrial electron transport chain that, when removed, decreases ATP production in the mitochondria and causes stunted growth, slow

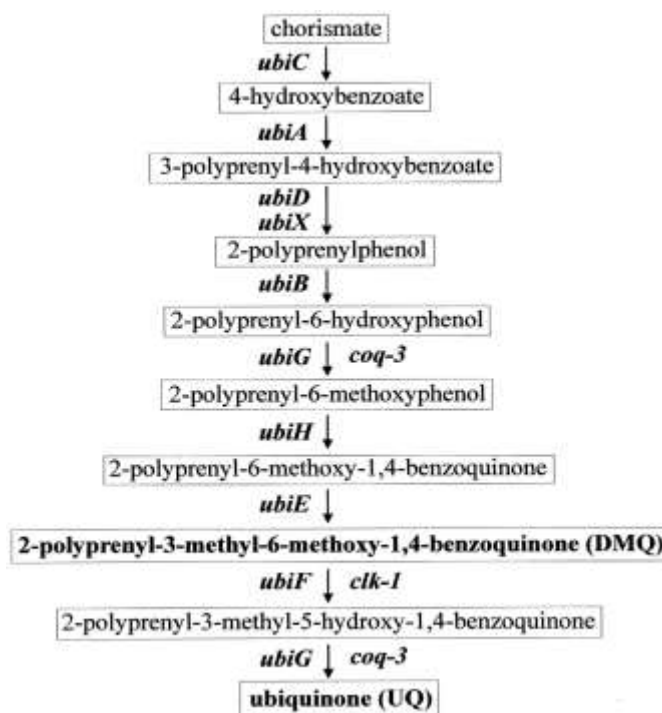


Figure. 2.1 Biosynthetic pathway of ubiquinone in mitochondria, showing metabolic mutant defects (Hihi et al., 2002)

movement and increased longevity in *C. elegans* (Hihi et al., 2002). Detailed mechanisms of the synthetic pathway can be seen in *Figure 2.1*.

*Coq-3* (*coq-3(ok506) IV/nT1 [qls51] (IV;V)*) is the second of the metabolic mutants, and lacks 3,4-dihydroxy-5-hexaprenylbenzoate methyltransferase, an enzyme analogous to COQ-3, a mitochondrial enzyme that is involved in the synthesis of coenzyme Q<sub>10</sub> (*Coq-3* (gene), n.d.). These worms were provided by the *C. elegans* Reverse Genetics Core Facility at the University of British Columbia. This specific mutation is sex-linked and dominant, so the heterozygous dominant worms are tagged with GFP for correct identification. Homozygous recessive worms are non-viable.

*Clk-1* and *coq-3* strains were chosen to investigate different knockout mutations of enzymes directly involved in the electron transport chain. Each deals with a separate part of the chain, but both directly influence coenzyme Q<sub>10</sub> and its ability to function properly in the electron transport chain. These strains, when compared with AD strains under the same conditions and given the same treatments will allow the team to investigate the possibility of metabolic disruptions in Alzheimer's Disease.

### **2.1.3 Heat Shock to Induce Mutations**

All strain of worms were initially grown at 20°C, then either eggs or L1 were passed onto new seeded plates. The amounts of worms that were passed onto these plates varied per assay being completed and were then placed into the 25°C incubator for 48-72 hours. After at least 36 hours, the plates were taken out of the incubator and placed on the benchtop for 30 minutes before any testing began. The worms were then passed to the testing plate and each of the given assays were performed. During the testing the time, the plate was placed back into the incubator if more than one assay was being performed from the initial plate. After the first test was completed, the seeded plate was once again taken out of the incubator and allowed to sit on the benchtop for 10 minutes before testing. This process was repeated until all viable animals on each plate was tested (Adapted from Coyle, Nikolaki, & Ong, 2016).

## **2.2 Addition of Derivatives to LB media and OP50**

### **2.2.1 Punicalagin**

In order to create a solution with a final concentration of  $1.2 \times 10^{-7}$  M punicalagin (Oladije et al., 2014) first 1.3 mg of punicalagin was weighed out using an analytical balance. This was then mixed 0.5 mL of 100% ethanol. After the powder was completely dissolved, then

99.5 mL of ultrapure MilliQ water was added to the same flask and mixed thoroughly. Then a 1:10 dilution was performed with 10 mL of this first solution being added to 90 mL of ultrapure MilliQ water. After this dilution was performed, 10 mL of the second solution was filter sterilized using a 0.2  $\mu$ M Steritop™ filter. Once sterile, a second 1:10 dilution was performed with the sterile 10 mL of the second solution and 90 mL of sterile, liquid LB media. This solution was then mixed thoroughly. This final solution was then inoculated with a single colony of OP50 *E. coli*, which was subsequently placed into a 37°C to incubate for a day. Once grown, this solution could then be seeded onto NGM plates and placed at room temperature to dry. All three solutions were then placed in the 4°C fridge until they were needed again.

### **2.2.2 Coenzyme Q<sub>10</sub>**

Using an analytical balance, 1.03 mg of Coenzyme Q<sub>10</sub> was weighed and then dissolved with 5 mL of 100% ethanol. This solution was then combined with 95 mL of ultrapure MilliQ water in order to achieve an initial concentration of  $1.2 \times 10^{-5}$  M. Then a 1:10 dilution was then performed with 10 mL of the initial solution and 90 mL of ultrapure MilliQ water. Once the second solution was mixed thoroughly, 10 mL was then filter sterilized using a 0.2  $\mu$ M Steritop™ filter. Once this solution was sterilized, it was then added to 90 mL of sterile, liquid LB media which would allow for a final concentration of  $1.2 \times 10^{-7}$  M to be achieved. Once this final solution was made, it was inoculated with a single colony from a plate of OP50 *E. coli* and placed into the 37°C warm room for a day. After the liquid culture was grown up it was used to seed NGM plates at room temperature until they were dry. The first two solutions were placed in the -20°C while the liquid culture was placed in the 4°C fridge until further use.

## **2.3 Assays**

### **2.3.1 Avoidance Assay**

Ten young adult worms are picked onto an unseeded plate and allowed to adjust to this plate for approximately 1 minute. After the adjustment time has ended, the testing can begin through the use of two different solutions and the drop method.

Glass capillaries are then pulled apart with the use of a flame to soften the glass, and in order to make it fine tipped. This is then fixed in the mouth pipetting apparatus. The fine tip, that is now connected to the mouth pipetting apparatus, as can be seen in *Figure 2.2*. The needle is then placed in one of the solutions to collect a sample of it.

A small drop is then placed near the tip of each tail of the forward moving worms. Capillary action then carries the solution up to the pharynx of the worm where one of two responses will be performed within 4 seconds after exposure to the solutions (Hilliard, Bargmann, & Bazzicalupo, 2002). An example of these responses can be seen in *Figure 2.3*. The first action, however, is a no avoidance response which is continued forward movement after the drop has been placed near the tail of the worm. While the second is an avoidance response which has three further classifications of an omega turn, full reversal, and a greater than 90° turn. Each strain was tested until an n of 10 had been achieved.

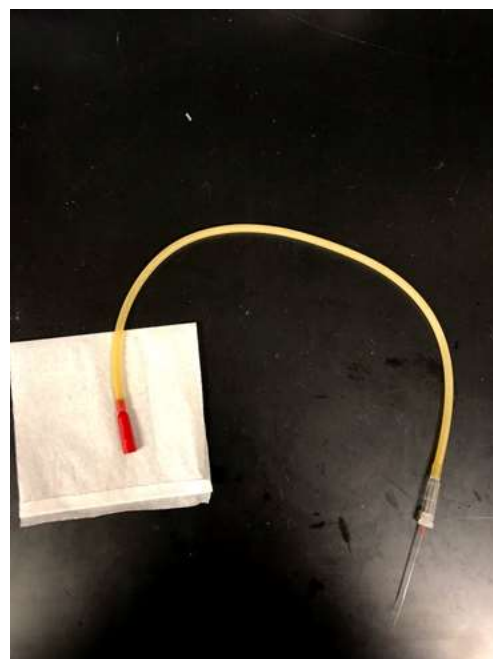


*Figure 2.2: A Mouth Pipette with a fine tipped needle used in Avoidance Assays. The red part is placed in the researchers mouth and liquid is taken up in the needle on the clear end. The tip is then placed near the tail end of the worm in order to gauge their avoidance behavior. (Picture created by: Consedine, 2018)*

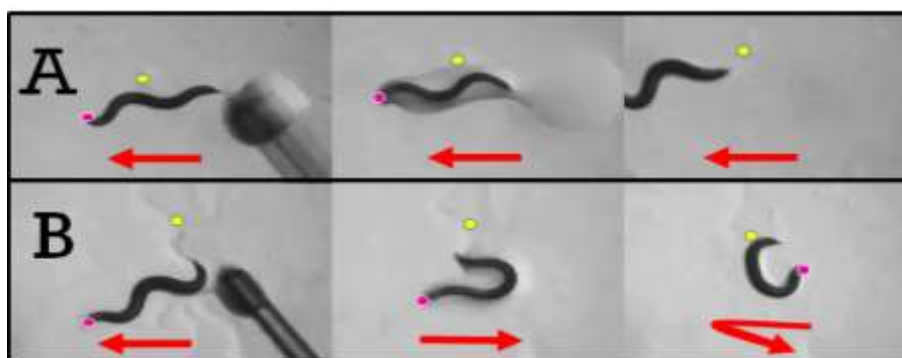


*Figure 2.3: A depiction of two different responses seen when testing the worms with the avoidance assay. A no avoidance response (A), typically seen with the solvent control, and an avoidance response (B), which would be seen with an experimental solvent, in the avoidance assay (Chute, 2013)*

For the purposes of this study, M9 buffer and 0.1% SDS were being used to test for the avoidance response for each assay plate. The 0.1% SDS was made by mixing 995  $\mu\text{L}$  of M9 buffer with 5  $\mu\text{L}$  of 20% SDS solution. M9 is a buffer solution that is used to wash *C. elegans* and this solution is being used as the solvent control. Sodium dodecyl sulfate, or more commonly known as SDS is a detergent typically used to denature proteins. In terms of *C. elegans*, however, it is a known repellent which should cause an avoidance response when exposed to this chemical. After each drop is applied to tail of each worm, the response is noted in a lab notebook for every plate tested. The avoidance index is then calculated for each solution by dividing the number of avoidance responses by the total of number of drops.

### 2.3.2 Chemotaxis Assay

One to two days prior, approximately 100 adult worms were transferred to a seeded OP50 *E. coli* NGM plate, and stored in the appropriate temperature, 16°C, or 25°C. All worms will be coming from the 16°C fridge, however this is the time to relocate the worms to the incubator for heat shock if necessary.

On an unseeded NGM plate, a dot was made at the center with a marker; this is the origin. Two small circles, D and C should be made 180° apart from each other around the edges as can be seen in *Figure 2.4*. On each of the dots 1  $\mu\text{L}$  of sodium azide was placed on them as this compound can be used as a paralytic. On spot D, 1  $\mu\text{L}$  of  $10^{-3}$  M diacetyl was added as well. On spot C, 1  $\mu\text{L}$  of  $\text{DiH}_2\text{O}$  should be added. The plates should remain covered as they dried.

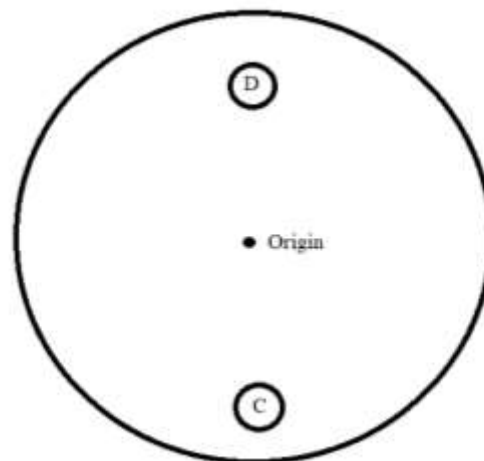


*Figure 2.4: Set up of Chemotaxis plate. D would be where diacetyl is added, C would be where water is added, and the origin is where the worms are added to the plate (Pictured created by: Randle, 2018).*

Using 1mL of S. Basal, a p1000 pipetman, wash the plate of worms, and transfer the wash to a 1.5mL microfuge tube. After 5-10 minutes, check that the worms have pelleted on the bottom of the tube, and aspirate off the remaining S. Basal. The worms in the tube should be washed

with S. Basal two more times, followed by one wash of water. The water does not need to be aspirated off.

On one of the plates prepared with the chemicals, 10 $\mu$ L of worms suspended in the water wash were added to the plate on the origin. The remaining water is dried off gently with the corner of a kimwipe. There should be enough worms in the centrifuge tube to load approximately five plates. Experimental plates with worms are returned to the fridge or incubator for about 45 minutes.

After 45 minutes of exposure to the chemicals, the plates are retrieved from the fridge or incubator and examined under a microscope. The number of worms at the chemical stimulus, spot D, are counted and noted in a lab notebook. The number of worms at the water control, spot C, are counted and recorded. The chemotaxis index is calculated by the following equation.

$$\text{Chemotaxis Index} = \frac{(\text{Worms at Stimulus} - \text{Worms at Control})}{\text{Total Worms}}$$

*Equation 2.1: Equation for calculating chemotaxis index*

### 2.3.3 Locomotion Assay

Tests were run with five worms per plate on 35mm NGM plates seeded with OP50 *E. coli* LB media. Testing plates were prepared the day before running the assay. The plate seeding takes place near an open flame, where 2-4 drops of OP50 *E. coli* are placed on the plate using a Pasteur pipet. A lawn spreader (a bent Pasteur pipet) is dipped in ethanol, flamed, and then used in conjunction with a plate spinner to spread the lawn to cover the agar surface. Test plates are left to dry overnight at 23°C.

Worms were prepared the night before or morning of the assay. Sixty to seventy adult worms were picked to a seeded holding plate and were maintained at the same culture temperature until the assay began. To begin the assay, five worms were picked from the holding plate and placed in the center of an NGM test plate. Once the worms were on the test plate, the plate was placed on the camera stage as seen in *Figure 2.5*. Using the nematode tracking software Wormlab' and the

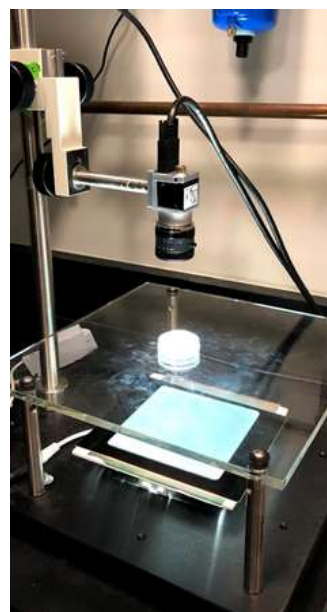


*Figure 2.5: An Example of the Testing Plate on the Camera Stage during an experiment (Pictured created by: Consedine, 2018)*

camera's lenses, the focus and lighting were adjusted to see the worms clearly and with high contrast. Frames per second was set to 7.5, the duration to 20 minutes, and the resolution as high as possible. The worm tracker program was run.

Once finished, the recording needed to be prepared, tracked and repaired. The recording was opened in Wormlab for processing, as seen below in *Figure 2.6*. Threshold was increased to 110-150 until all worms were highlighted in green, and the labeling tool was used to draw an oval in the non-highlighted portion of the agar. This restricted the tracking software to inside the label, to cover as much space as possible without touching green. The pen tool was used to individually label each worm, and tracking was restricted to the labeled region. At this point, each file would be ready for tracking, which could be done one recording at a time or sequentially, with a batch of multiple files.

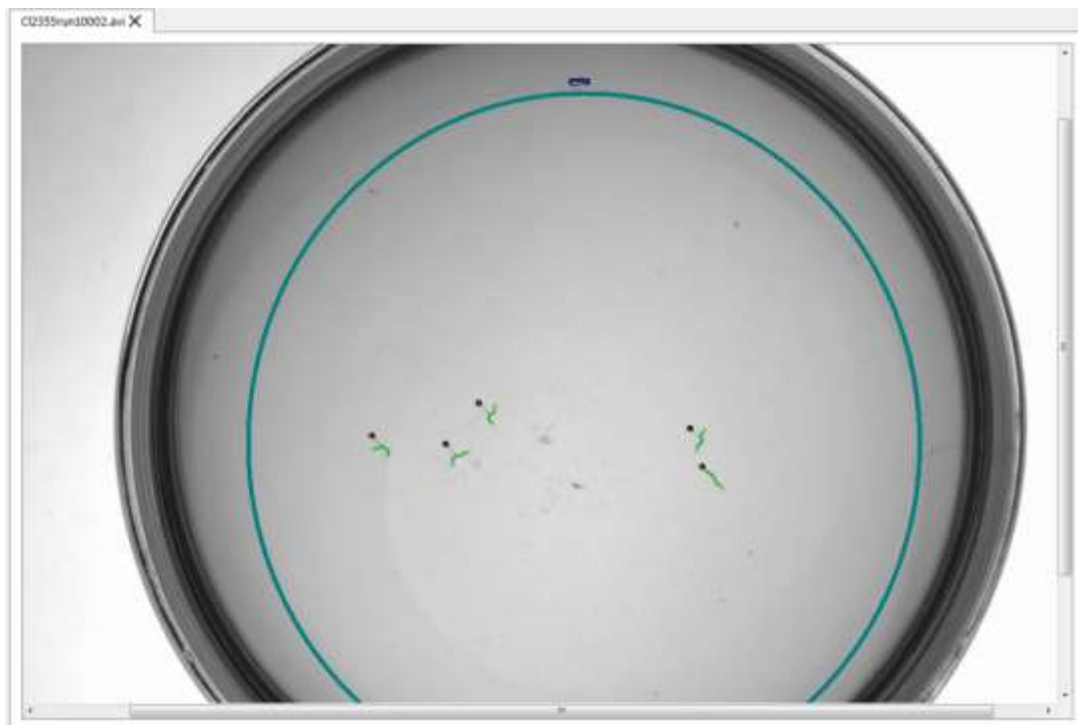


*Figure 2.6: An Example of the WormLab Software tracking five adult worms, marked in green, during an experiment (Pictured created by: Consedine, 2018)*

### **2.3.4 ATP Bioluminescence Assay**

The following procedure was adapted from *Intracellular Assessment of ATP Levels in Caenorhabditis elegans* by Palikaras and Taveranakis. From each treatment and temperature group, a full plate of adult worms of each species were washed off of a plate into a 1.5mL eppendorf tube with 1.5 mL of M9 buffer. Once in the eppendorf tube, they were allowed to sit

for 15 minutes until a “pellet” of worms formed at the bottom of the tube. Then 1 mL of this M9 was taken out of the tube and disposed of. Once completed. Another 1 mL of M9 was added to the tube and again the tube was allowed to sit for an additional 15 minutes. Once this second wash was completed, 1450  $\mu$ L was taken out and disposed of appropriately. Using liquid nitrogen, the tubes were flash frozen with liquid nitrogen and then stored in the -80C freezer until the day of the assay (Palikaras & Tavernarakis, 2017).

When it is time to assay the worm samples for measurement, the frozen samples should be immersed in boiling water for 15 minutes, and then immediately incubated on ice for 5 minutes. Using a temperature controlled centrifuge, the tubes should be centrifuged at 14,800 x G for 10 minutes at 4°C. The supernatant was then transferred to a new 1.5mL tube. The supernatant was diluted using a 10 fold dilution. The diluted samples were stored in the -20°C until the time of the assay, and kept on ice while in use.

An ATP Bioluminescence Assay Kit was purchased from Roche Scientific, and all chemicals were prepared according to the kit. 100uL of ATP standard, and M9 blank, and of each sample were loaded into individual 1.5mL tubes. The samples in the 1.5 mL tubes are transferred to an individual wells in a 96-well plate. Once all of them were added, 100  $\mu$ L of luciferase is added to each sample as seen in *Figure 3.7*.

Once the samples and luciferase have been added to the well, the plate is placed in the PerkinElmer 2300 plate reader as seen in *Figure 3.8* and the luminescence levels are read. This was repeated until all the samples have been measured. Luminescence and ATP levels are



*Figure 2.7: An example on how one would load the 96-well plate with either a sample or luciferase for the ATP bioluminescence assay. An researcher will place the pipette tip on the edge of the well and add the sample/enzyme to that well by pressing on the top of the micropipette. (Pictured created by: Consedine, 2018)*

directly correlated when using luciferase, meaning the higher the level of luminescence indicated the higher the amount ATP in the sample. This was repeated three times for each sample type for an n of 3 for each (Palikaras & Tavernarakis, 2017).



*Figure 2.8: An example on how the plate reader would be placed in the PerkinElmer 2300 plate reader. A researcher would then close the lid and run the program. After about thirty seconds, the researcher would have the luminescence values for each sample (Pictured created by: Consedine, 2018).*

### 3. Results and Discussion

Following the methodology discussed above, the four different assays (the avoidance assay, the chemotaxis assay, mobility assay, and the ATP Bioluminescence assay) were performed on the five different strains of *C. elegans*. The strains were grown on the following conditions: OP50 *E. coli*, OP50 + Punicalagin, and OP50 + Coenzyme Q<sub>10</sub>. The results for these assays are reported throughout this chapter.

#### 3.1 Baseline testing

The baseline was obtained by testing the wild-type (N2), the transgenic Alzheimer's Disease models CL2355 (pan-neuronal A $\beta$  expression) and CL4176 (pan-muscular A $\beta$  expression), and the metabolic mutant strains (*coq-3*, *clk-1*) in all four of the assays. The worms in this case were grown on NGM plates with OP50 *E. coli*.

##### 3.1.1 Avoidance Assay

The avoidance assays tests the chemosensory abilities of these worms when exposed to a particular, aversive stimulus. In this assay only the N2, CL2355, *coq-3*, and *clk-1* strains were tested. In this case all the worms were tested with 0.1% SDS as the aversive compound. *Figure 3.1* shows all the strains at both 16°C and 25°C when grown on untreated OP50. When testing the N2 worms grown at 16°C, the average avoidance index was  $0.84 \pm 0.030551$  while testing the same strain at 25°C resulted in an average avoidance index of  $0.83 \pm 0.03$ . At both temperature conditions the *coq-3* and *clk-1* mutants each yielded similar average avoidance index values to wild-type worms. At 16°C, *coq-3* and *clk-1* both yielded a value of  $0.79 \pm 0.01795$ . At 25°C, *coq-3* produced an average avoidance index of  $0.82 \pm 0.02$  while *clk-1* gave a value of  $0.82 \pm 0.01333$ .

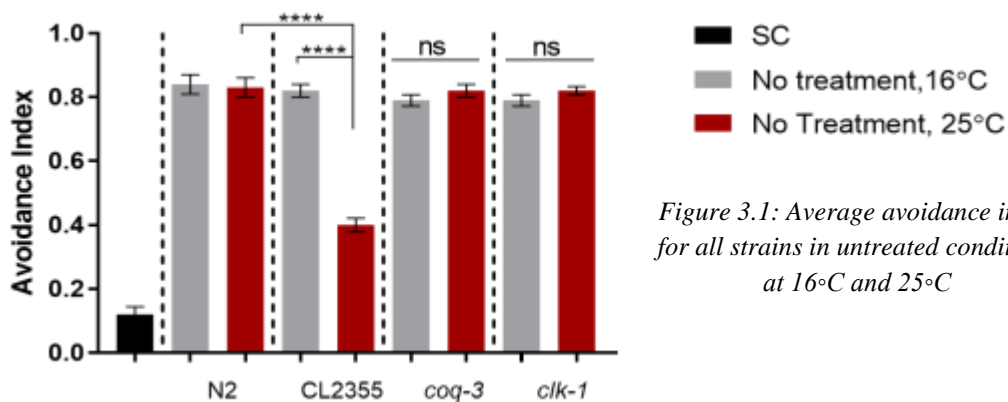


*Figure 3.1: Average avoidance index for all strains in untreated conditions at 16°C and 25°C*

These values show that there was no observed aversive chemosensory deficit in either of the metabolic mutants when compared to wild-type values at either temperature when grown on untreated OP50. A defect was evident when the CL2355 AD model was tested. At 16°C this

strain produced a normal avoidance index of  $0.82 \pm 0.02$ . However, at  $25^{\circ}\text{C}$ , the CL2355 yielded an average avoidance index of  $0.4 \pm 0.021082$  ( $p < 0.0001$ ). This value indicates that there is an apparent chemosensory defect when this particular strain is propagated at  $25^{\circ}\text{C}$ . This conveys that at this temperature the  $\text{A}\beta_{42}$  is hydrolyzed which results in chemosensory deterioration. This leads to a loss of response when exposed to an aversive stimulus such as SDS.

### 3.1.2 Chemotaxis Assay

The chemotaxis assay, like the avoidance assay, also tests the chemosensory ability of the worms, however, it instead tests the attraction to a chemical stimulus. The N2, CL2355, *clk-1*, and *coq-3* worms were tested with  $10^{-3}$  M diacetyl as the chemical attractant. Like the avoidance assay, the chemotaxis assay tested worms at both  $16^{\circ}\text{C}$  and  $25^{\circ}\text{C}$ . The results of the chemotaxis assay at  $16^{\circ}\text{C}$  and

$25^{\circ}\text{C}$  can be seen in figure 3.2. The

wild-type N2 worms had a chemotaxis index of  $0.512 \pm 0.0346$  at  $16^{\circ}\text{C}$  and  $0.726 \pm 0.0558$  at  $25^{\circ}\text{C}$

( $p=0.0027$ ) The

increase in chemotaxis index that is observed with the increase of temperature is due to the increased biochemical processes of the worms at higher temperatures. The CL2355 transgenic AD worms had a chemotaxis index of  $0.474 \pm 0.0511$  at  $16^{\circ}\text{C}$  and  $0.305 \pm 0.0529$  at  $25^{\circ}\text{C}$  ( $p < 0.0001$ ,  $p=0.0248$ ). The *clk-1* metabolic mutant worms have a chemotaxis index of  $0.403 \pm 0.0247$  at  $16^{\circ}\text{C}$  and  $0.489 \pm 0.6545$  at  $25^{\circ}\text{C}$  ( $p=0.0183$ ). The *coq-3* metabolic mutant worms have a chemotaxis index of  $0.389 \pm 0.0467$  at  $16^{\circ}\text{C}$  and  $0.454 \pm 0.0622$  at  $25^{\circ}\text{C}$  ( $p=0.0061$ ). Both of these strains experience a small increase in chemotaxis index as the temperature increases, as was observed in the N2 strain, however, this shift is not statistically significant.

The observed chemotaxis index for the CL2355 worms decreases as the temperature increases. The increasing temperature results in the full expression of the  $\text{A}\beta$  protein that is expressed in this transgenic strain when exposed to heat. The full expression of the  $\text{A}\beta$  results in

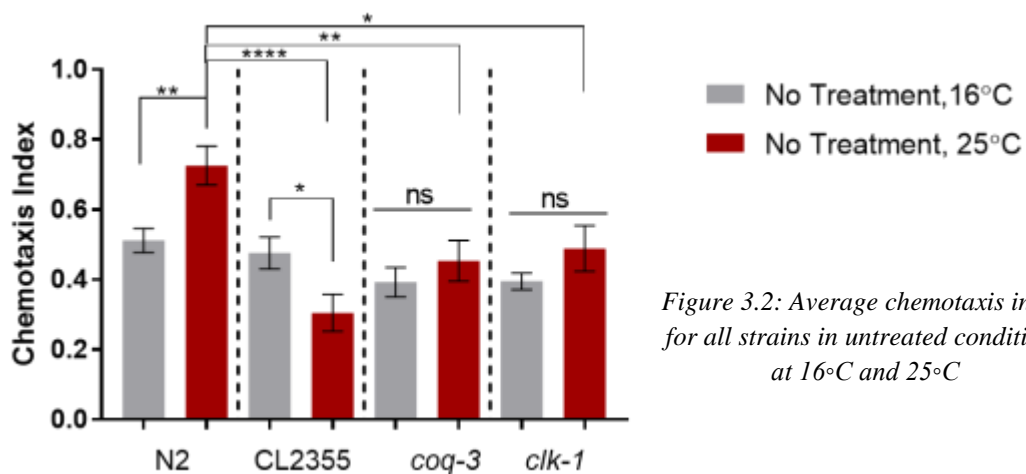


Figure 3.2: Average chemotaxis index for all strains in untreated conditions at  $16^{\circ}\text{C}$  and  $25^{\circ}\text{C}$

the phenotype of decreased chemotaxis. The metabolic worms experience an overall deficit in chemotaxis index due to the lack of energy being produced, and thus lack of energy available for neuronal activity. The lack of energy production causes a decreased energy use. The chemotaxis assay looks specifically at neuronal activity, and a decrease chemotaxis index is indicative of decreased neuronal activity.

### 3.1.3 Mobility Assay

The mobility assay measures average speed of five worms on an OP50 seeded NGM plate with no stimulus over the course of 20 minutes. These results are displayed in *Figure 3.3* below. Wild-

type N2 worms grown at 16°C measured a speed of  $80.24 \pm 3.826 \mu\text{m/s}$ , and at 25°C they were

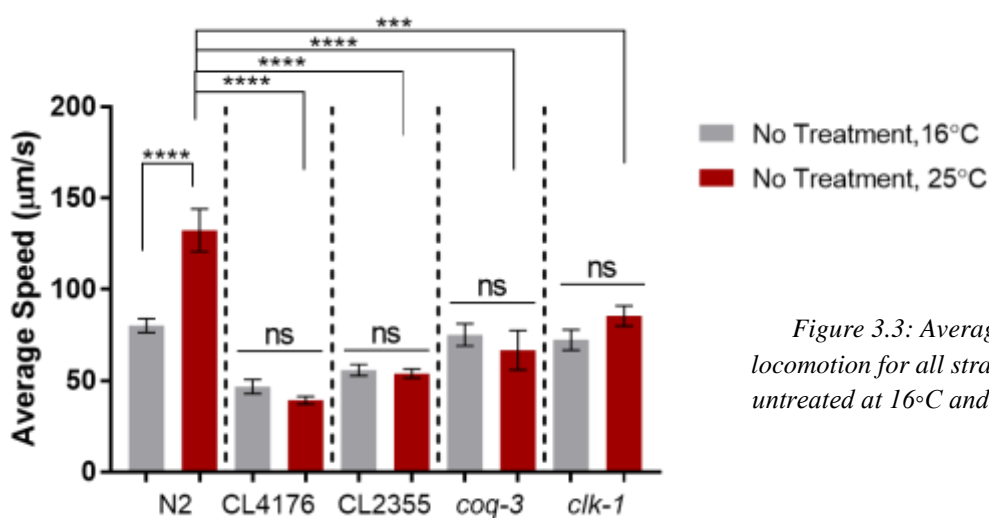


*Figure 3.3: Average locomotion for all strains in untreated at 16°C and 25°C*

measured at  $123.40 \pm 11.68 \mu\text{m/s}$  ( $p < 0.0001$ ). This increase in mobility is due to the aforementioned increased metabolic rate when worms are grown at higher temperatures. The AD transgenic pan-muscular strain (CL4176) exhibited significantly impaired locomotion, with an average speed of  $46.81 \pm 3.826 \mu\text{m/s}$  ( $p = 0.0027$ ) when grown at 16°C and  $39.36 \pm 2.03 \mu\text{m/s}$  ( $p < 0.0001$ ) when grown at 25°C. Similarly, the pan-neuronal AD strain CL2355 measured a speed of  $55.83 \pm 3.42 \mu\text{m/s}$  ( $p = 0.0269$ ) at 16°C and  $53.88 \pm 2.81 \mu\text{m/s}$  ( $p < 0.0001$ ) at 25°C. Unlike the wild-type strain, the two AD strains showed a decrease in speed when grown at 25°C versus 16°C. The metabolic mutant *clk-1* showed no significant change from wild-type with a speed of  $72.39 \pm 5.58 \mu\text{m/s}$  at 16°C, but had an average speed of  $85.53 \pm 5.55 \mu\text{m/s}$  ( $p = 0.0003$ ) when grown at 25°C, notably lower than N2 at 25°C. Like *clk-1*, *coq-3* had a near wild-type mobility of  $75.14 \pm 6.67 \mu\text{m/s}$  at 16°C. Interestingly, *coq-3* exhibited a drop in mobility at 25°C to  $47.54 \pm 2.35 \mu\text{m/s}$  ( $p < 0.0001$ ), not unlike the AD worms' results.

Both AD strains' levels of A $\beta$  expression are temperature dependent, so increased growth temperature causes high levels of expression which negatively affects mobility. This explains why neither strain speeds up to same degree as N2. Additionally, *coq-3* showed a drop in mobility--this effect is probably due to general energy deficiency as a result of the mutation in energy transduction pathways. It may not be severe enough to cause a drop in low temperature growth conditions, but the deficit is exacerbated when worms are heat shocked. As other biological enzymes become more efficient, the mutated enzyme remain inactive, creating the possibility for bottlenecks and overproduction, ultimately slowing the worm's movement.

### 3.1.4 ATP Bioluminescence Assay

The ATP Bioluminescence Assay measures the amount of ATP in a particular mass of worms. All worm strains were tested for this assay and they were grown at both testing temperatures, similar to the other three assays. A visual representation of this data can be seen in *Figure 3.4*. When tested the wild-type worms (N2) had a calculated concentration of ATP of  $142.4 \pm 52.66 \mu\text{M}$  at  $16^\circ\text{C}$ . While at  $25^\circ\text{C}$  this same strain had an ATP concentration of  $109.3 \pm 20.26 \mu\text{M}$ . The *coq-3* strain gave expected results for this assay at both temperatures. At  $16^\circ\text{C}$  these worms produced an ATP concentration of  $152.9 \pm 19.78 \mu\text{M}$  and at  $25^\circ\text{C}$  these same worms yielded a value of  $83.73 \pm 11.53 \mu\text{M}$  ( $p=0.0129$ ). However at  $16^\circ\text{C}$ , the *clk-1* worms yielded a value of  $285.3 \pm 71.27 \mu\text{M}$  and at the temperature upshift the resulting concentration was  $138.5 \pm 33 \mu\text{M}$ . A similar trend is once again observed in these worms as with the *coq-3* strain. The

temperature upshift condition in the *coq-3* worms resulted in a much lower concentration

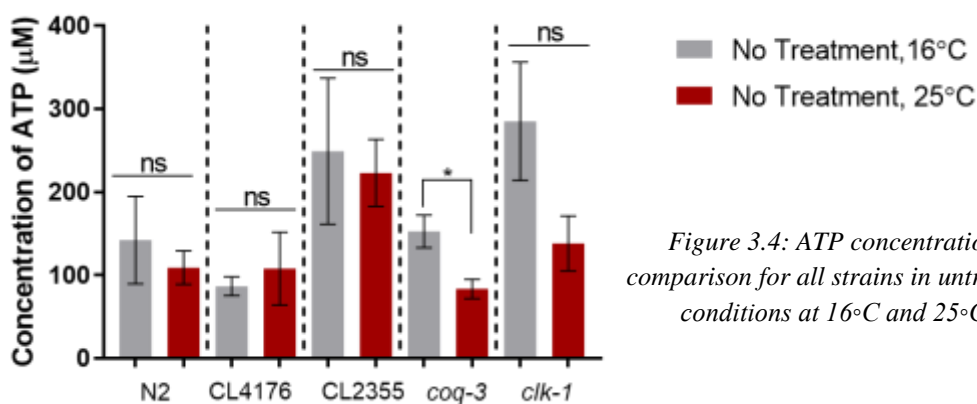


*Figure 3.4: ATP concentration comparison for all strains in untreated conditions at  $16^\circ\text{C}$  and  $25^\circ\text{C}$*

of ATP than at  $16^\circ\text{C}$ . Both of these strains decreased at the higher temperature, in a similar manner that N2 does. This is indicating that at this higher temperature that all of these trains are

using more ATP than at the lower one. This suggests that all of their process on a cellular level would be sped up as a result of being grown at increased temperatures

For the muscular AD model (CL4176), the measured values given at both temperatures were approximately the values of the N2 strain. These concentrations are as follows: at 16°C CL4176 yielded a value of  $86.94 \pm 11.29 \mu\text{M}$  and at 25°C they produced  $108 \pm 43.73 \mu\text{M}$ . Conversely, the pan-neuronal AD model (CL2355) produced surprisingly higher values at both temperatures. At 16°C, these worms produced an ATP concentration of  $249.3 \pm 87.79 \mu\text{M}$ . While at the temperature upshift, CL2355 then yielded a value of  $223.3 \pm 40.07 \mu\text{M}$ . The CL4176 strain produced a slight increase in ATP levels, however, its calculated values are similar to the N2 values.

The pan-neuronal AD model yielded approximately twice the amount of ATP compared to the wild-type at both temperatures. Based on this information, it can be suggested that the A $\beta$ <sub>42</sub> peptide is causing an overproduction of ATP within the organism. As this concentration is seen at both temperatures, it can then be assumed that the A $\beta$  protein is not completely silenced at 16°C in either strain as well. The metabolic mutant worms both measured ATP concentrations approximately equal to the wild type worms even though the worms are mutated to disrupt ATP production. This was unexpected, but it must be noted that the assay only measures the momentary ATP concentration at a single point in time in a worm. This concentration is a function of both the rates of ATP production and use, and is not necessarily entirely indicative of either. However, it does give the experimenter a window into the general trends of the ATP-producing metabolic processes and the opportunity for rough analysis.

### **3.2 Punicalagin Treatment**

To assess the effects of the potential therapeutics ability of punicalagin on both the AD transgenic models and metabolic mutants, all the worms were grown on plates with OP50 *E. coli* and punicalagin. These worms were then tested using the same experiments as before to see if this treatment was able to rescue the worms to normal behavioral phenotypes.

#### **3.2.1 Avoidance Assay**

The same avoidance assay was used to test the worm's avoidance response abilities when grown on OP50 *E. coli* and punicalagin at two different temperatures (16°C and 25°C). In the normal OP50 avoidance assay, it was observed that there was no significant difference between any of the strains when grown at 16°C, as can be seen in *Figure 3.5*. This same phenomenon was

again observed in this 16°C avoidance assay. They produced the following results as a result when tested with 0.1% SDS: N2 produced an avoidance index of  $0.79 \pm 0.0314$ , CL2355 displayed a result of  $0.85 \pm 0.0342$ , *clk-1* showed an avoidance index of  $0.79 \pm 0.0233$ , and *coq-3* had a result of  $0.84$

$\pm 0.0339$ . All of these values were expected to be similar as the untreated avoidance assays and were used as a control to make sure that the

punicalagin treatment was not having any additional, aversive effects on the worms.

Previously, the 25°C avoidance assays showed that CL2355 had a significant decrease in avoidance response behavior. While the other two mutants being tested, *clk-1* and *coq-3*, had a normal behavioral phenotype before treatment. Due to this the focus for this assay was to see if we could restore the CL2355 strain to the normal, wild-type avoidance behavior and see if there were any additional effects observed in the three other strains. The wild-type strain was tested once again as a control and produced an avoidance response of  $0.82 \pm 0.0249$ , as can be seen in Figure 3.6. The *clk-1* and *coq-3* mutants again produced avoidance indices at approximately the wild-type levels of

$0.78 \pm 0.0326$  and  $0.79 \pm 0.0344$ .

When tested in the avoidance assay, the CL2355 worms produced a result of  $0.83 \pm 0.0260$  ( $p < 0.0001$ ).

This shows that through

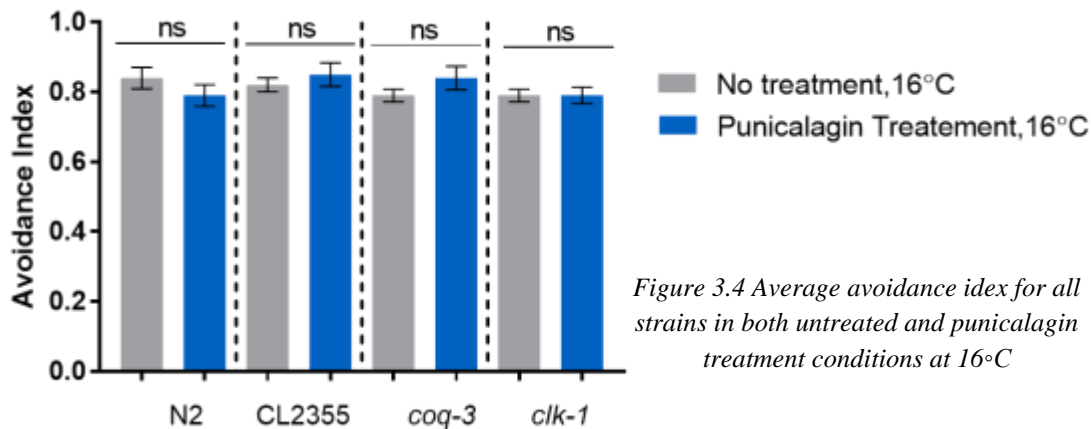


Figure 3.4 Average avoidance index for all strains in both untreated and punicalagin treatment conditions at 16°C

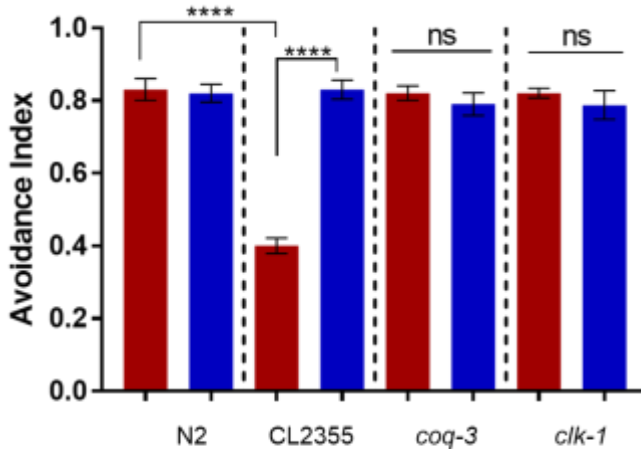


Figure 3.6: Average avoidance index for all strains in both untreated and punicalagin treatment conditions at 25°C

■ No Treatment, 25°C  
 ■ Punicalagin Treatment, 25°C

preventative treatment measures with a polyphenol such as punicalagin we were able to alleviate the effects of  $A\beta_{42}$ . Typically, these worms have detrimental chemosensory ability, however, when treated with punicalagin were able to restore the CL2355 model to normal chemosensory function, rescuing the avoidance phenotype of the CL2355 worms.

### 3.2.2 Chemotaxis Assay

The Chemotaxis index of the worms was also measured at 16°C and 25°C after the worms were

treated with punicalagin, these results can be seen in *figure 3.7*. At 16°C, the N2 worms experienced an increase, compared to

untreated N2 worms at 16°C, in attractive chemosensory ability, showing a chemotaxis index of  $0.602 \pm 0.0563$ . There was a slight increase in attractive chemosensory ability at 25°C, compared to 16°C, punicalagin treatment, producing a chemotaxis index of  $0.621 \pm 0.0573$ . This decrease is not a significant decrease and could be due to giving a healthy worm treatment that it does not need.

The chemotaxis index for the CL2355 strain remained constant, when exposed to punicalagin, at 16°C, measuring  $0.462 \pm 0.0432$ . There was a significant increase from the previously observed values at 25°C in attractive chemosensory ability, with a chemotaxis index of  $0.699 \pm 0.0680$  ( $p=0.0002$ ). Both the *clk-1* and *coq-3* mutant worms experienced increases in chemotaxis index, compared to no treatment, at both temperature conditions. For punicalagin treatment at 16°C, the *clk-1* and *coq-3* had chemotaxis indexes of  $0.517 \pm 0.0539$  ( $p=0.0448$ ) and

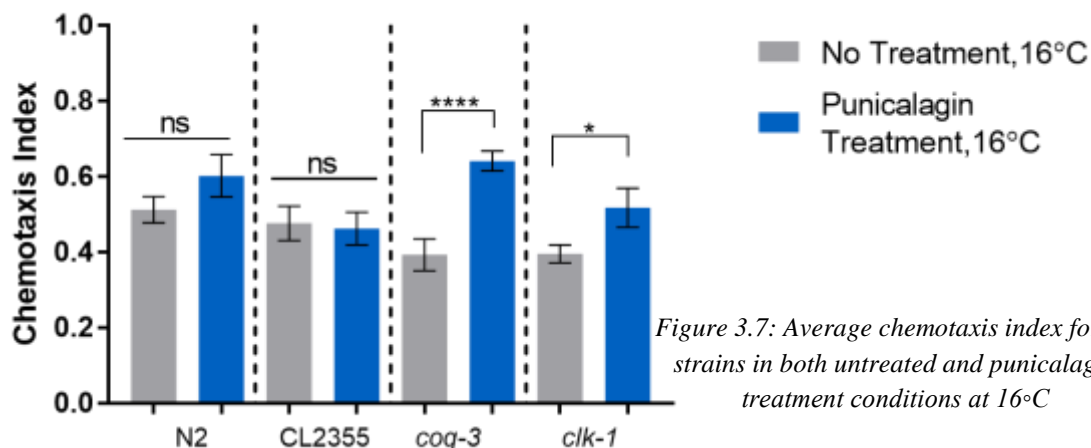


Figure 3.7: Average chemotaxis index for all strains in both untreated and punicalagin treatment conditions at 16°C

$0.634 \pm 0.0288$  ( $p < 0.0001$ ), respectively. At  $25^{\circ}\text{C}$ , *clk-1* had a chemotaxis index of  $0.704 \pm$

$0.0395$

( $p = 0.0105$ )

while *Coq-3*

had a

chemotaxis

index of  $0.716$

$\pm 0.0554$

( $p = 0.0043$ ).

When

given punicalagin as a dietary supplement, the attractive chemosensory ability in the Alzheimer's Disease models and metabolic mutants of *C. elegans* was able to be rescued to the untreated, wild-type chemotaxis index of *C. elegans*. From previous research, we knew punicalagin was able to rescue the chemotaxis phenotype in Alzheimer's model worms. This set of assays was able to show punicalagin's positive effect on the metabolic mutants. Because of these observed rescues, we can also conclude that punicalagin is working in the ETC of the CL2355 strain.

### 3.2.3 Mobility Assay

Worms treated with punicalagin were tested on standard OP50 seeded NGM plates. N2 worms on punicalagin at  $25^{\circ}\text{C}$  showed a slight decrease to  $97.84 \pm 12.01 \mu\text{m/s}$  ( $p = 0.0267$ ) compared to untreated worms, and N2 worms on punicalagin grown at  $16^{\circ}\text{C}$  move at  $80.24 \pm 3.83 \mu\text{m/s}$ , as seen in *Figure 3.9* and *3.10*. Pan-muscular transgenic AD strain CL4176 grown on punicalagin showed a partial rescue in mobility, with an average speed of  $52.84 \pm 3.43 \mu\text{m/s}$  ( $p < 0.0001$ ,  $p = 0.0004$ ) at  $25^{\circ}\text{C}$ , and a small increase at  $16^{\circ}\text{C}$  from untreated to  $64.35 \pm 2.81 \mu\text{m/s}$  ( $p = 0.0017$ ). However, the pan-neuronal transgenic AD strain CL2355 grown on punicalagin at  $25^{\circ}\text{C}$  showed no significant rescue at  $60.48 \pm 1.65 \mu\text{m/s}$  ( $p < 0.0001$ ,  $p = 0.0482$ ), but CL2355 at  $16^{\circ}\text{C}$  showed a slight increase to  $78.10 \pm 4.69 \mu\text{m/s}$  ( $p = 0.0009$ ). The metabolic strain *clk-1* showed a drop in speed with punicalagin at  $25^{\circ}\text{C}$  to an average of  $58.95 \pm 2.82 \mu\text{m/s}$  ( $p = 0.001$ ,  $p = 0.0019$ ), and no change from untreated at  $16^{\circ}\text{C}$  with a speed of  $76.73 \pm 5.41 \mu\text{m/s}$ . Conversely, *coq-3* mutants on punicalagin moved faster than untreated worms, with a treated

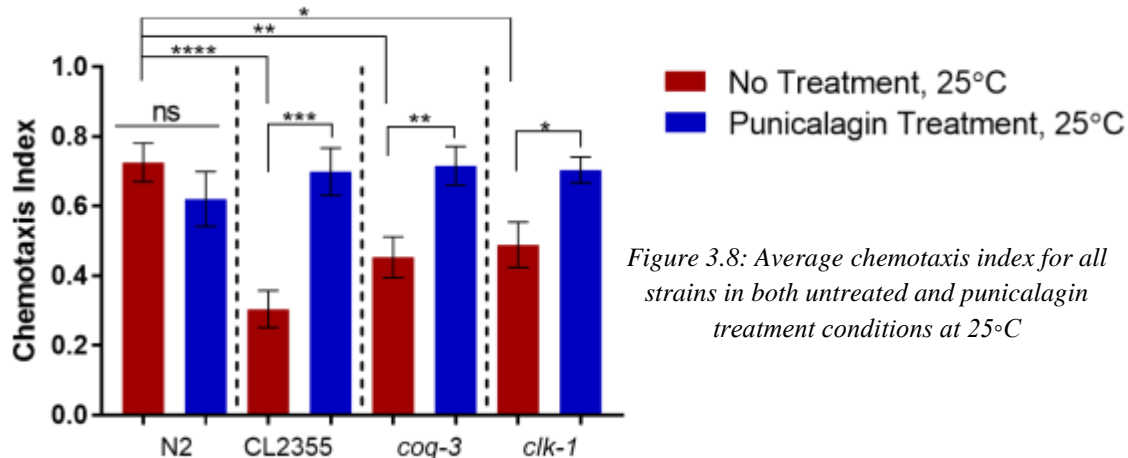


*Figure 3.8: Average chemotaxis index for all strains in both untreated and punicalagin treatment conditions at  $25^{\circ}\text{C}$*

speed of  $72.60 \pm 8.64 \mu\text{m/s}$  ( $p < 0.0001$ ) at  $25^\circ\text{C}$ , and an increase at  $16^\circ\text{C}$  to  $97.64 \pm 4.83 \mu\text{m/s}$  ( $p = 0.0093$ ).

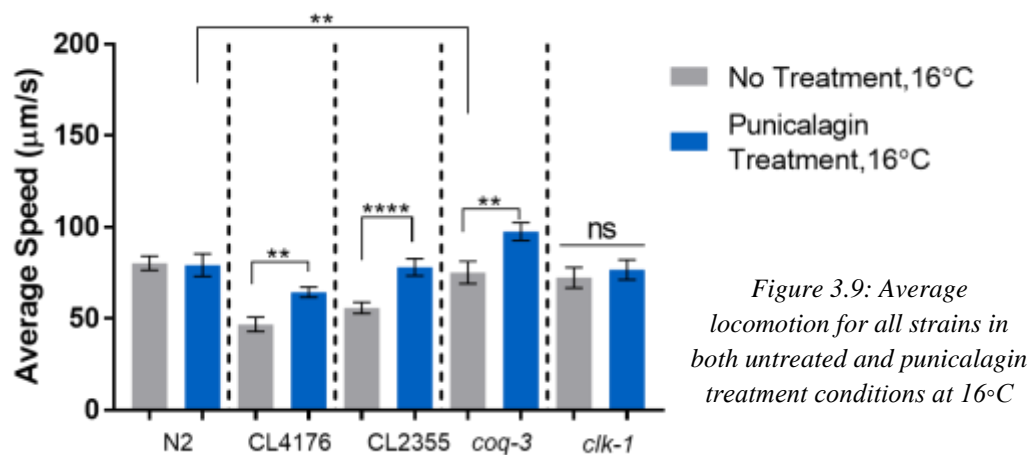


Figure 3.9: Average locomotion for all strains in both untreated and punicalagin treatment conditions at  $16^\circ\text{C}$

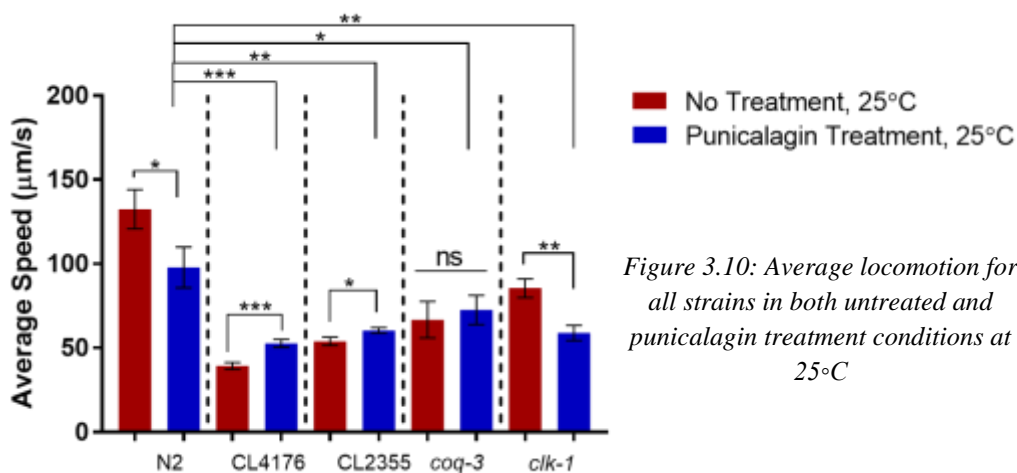


Figure 3.10: Average locomotion for all strains in both untreated and punicalagin treatment conditions at  $25^\circ\text{C}$

Although chemosensation in the AD models was successfully rescued by punicalagin at  $25^\circ\text{C}$ , general locomotion seems to be unaffected in the pan-neuronal model worms when  $\text{A}\beta$  is not fully expressed. Punicalagin seems to have a beneficial effect on the pan-muscular mutant, suggesting that the compound may be relevant in regards to the muscular atrophy aspects of Alzheimer's

disease. However, it did not rescue the wild-type phenotype of normal movement, as rolling behavior was still observed and worms traveled in small circles. Finally, both metabolic mutants exhibited opposite reactions when treated with punicalagin. This indicates that the drug may have an effect on energy transduction pathways which is observable in general locomotion.

### 3.2.4 ATP Bioluminescence Assay

Based on the results to the behavioral assays above, we then wanted to see the effect of punicalagin treatment on ATP production in all of the strains. When treated with punicalagin there were several differences observed at both the testing temperatures. These differences can be observed in *Figures 3.11 and 3.12*. At  $16^\circ\text{C}$  the N2 worms tested had an increased ATP

concentration of  $207.2 \pm 104.3 \mu\text{M}$  when given the punicalagin supplement. However when grown at  $25^\circ\text{C}$  the wild-type strain had almost the exact same concentration as the untreated condition. This concentration was measured to  $109.5 \pm 26.05 \mu\text{M}$ .

The metabolic worms produced surprising results at both temperature conditions. The *coq-3* strain produced a tremendous increase in the amount of ATP present when treated with

punicalagin at

both

temperatures.

These worms

had a

concentration

of  $555.6 \pm$

$161.05 \mu\text{M}$

( $p=0.0146$ ) at

$16^\circ\text{C}$  while at  $25^\circ\text{C}$  they produced a concentration of  $217.4 \pm 56.58 \mu\text{M}$  ( $p=0.0432$ ). The *clk-1*

produced differing results when given the treatment at either temperature. At  $16^\circ\text{C}$  this strain had

an ATP concentration of  $403.2 \pm 56.58 \mu\text{M}$  ( $p=0.0146$ ) when given the treatment. While at  $25^\circ\text{C}$

the concentration was calculated at  $82.35 \pm 18.44 \mu\text{M}$  ( $p=0.0432$ ). The transgenic AD models

produced both differing and similar results. At  $16^\circ\text{C}$ , the pan-muscular model CL4176 increased

while the pan-neuronal model CL2355 had a decrease in ATP production when given the

treatment. However, at  $25^\circ\text{C}$  both of these models had a significant decrease in ATP production.

The pan-muscular AD model produced concentrations of  $154.8 \pm 30.62 \mu\text{M}$  and  $42.96 \pm 6.957$

$\mu\text{M}$  at  $16^\circ\text{C}$  and  $25^\circ\text{C}$ , respectively. The CL2355 strain had a measured ATP concentration of

$151.5 \pm 19.04 \mu\text{M}$  at  $16^\circ\text{C}$ , and  $73.24 \pm 20.17 \mu\text{M}$  ( $p=0.0121$ ) at  $25^\circ\text{C}$ .

These results indicate that the treatment with punicalagin acts differently in each of the strains used. For the *coq-3* mutant, the high values recorded suggest a massive overproduction of

ATP and the coincidental misuse of ATP, as evidenced by the consistently low locomotion

values. The *clk-1* mutants experience an increase of ATP at  $16^\circ\text{C}$ , but a decrease at  $25^\circ\text{C}$ . The

treatment may be working to increase ATP production in the metabolic worms, but at higher

temperatures the worms use more energy, thus resulting in a lower ATP concentration. These

results also show that amount of the ATP in both of the AD models can be reduced through the

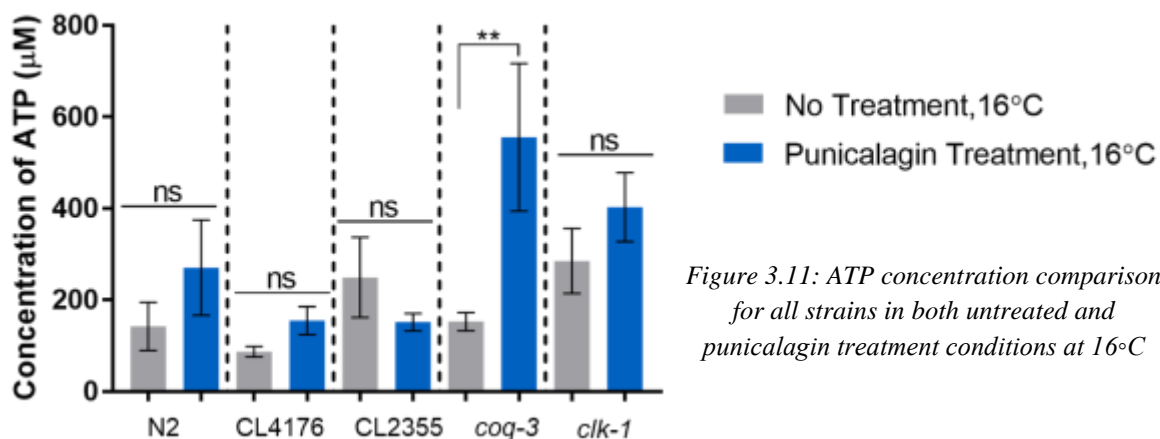


Figure 3.11: ATP concentration comparison for all strains in both untreated and punicalagin treatment conditions at  $16^\circ\text{C}$

use of punicalagin as a treatment. Specifically it shows that the severe overproduction of ATP in the CL2355 strain observed under untreated conditions at 25°C can be significantly reduced once given this

treatment. This indicates that another consequence of A $\beta$  may be alleviated through the use of this

polyphenol as a form of treatment. However, for the CL4176 strain due to low amount of A $\beta$  expression at 16°C this data suggests that this compound is causing the organism to slightly overproduce the amount of ATP compared to the wild-type levels.

### 3.3 Coenzyme Q<sub>10</sub>

In a similar manner to the assays tested with punicalagin, all the strains (N2, CL2355, CL4176, *clk-1*, and *coq-3*) were grown on OP50 *E. coli* with Coenzyme Q<sub>10</sub>. This happened at both temperatures in order to evaluate the effects of Coenzyme Q<sub>10</sub> as a potential therapeutic measure for both Alzheimer's Disease and general metabolic disorder. This was also done to see if we could rescue the strains to normal behavioral phenotype.

#### 3.3.1 Avoidance Assay

This assay was again administered in the same way that was stated in the methodology and in the other sections in this section. The 16°C discussed previously showed that all the strains (N2, CL2355, *clk-1*, and *coq-3*) had the same approximate avoidance index. However, in order to see if Coenzyme Q<sub>10</sub> had any additional effects, all the strains were tested when maintained at 16°C, the temperature in which no deficits are observed by any of the strains in a no treatment condition. The results from this assay at 16°C can be seen in *Figure 3.13* and *Figure 3.14*. When treated with Coenzyme Q<sub>10</sub>, N2 producing an avoidance index of  $0.82 \pm 0.0327$ . The other strains all produced similar values for this assay. The CL2355 strain generated an average avoidance index of  $0.88 \pm 0.0291$ . While the two metabolic mutants, *clk-1* and *coq-3*, had an avoidance index value of  $0.82 \pm 0.0294$  and  $0.81 \pm 0.0314$  respectively. All of these

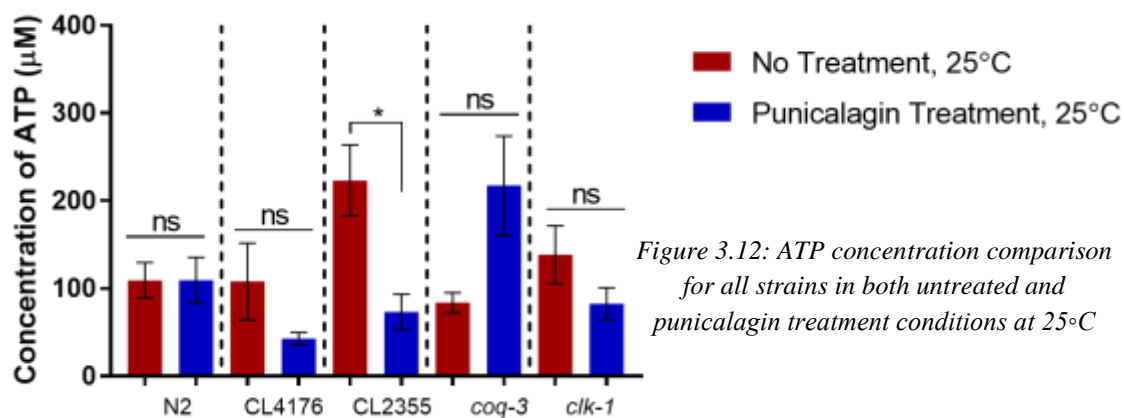


Figure 3.12: ATP concentration comparison for all strains in both untreated and punicalagin treatment conditions at 25°C

values were expected to be around these values and showed that the coenzyme Q<sub>10</sub> treatment was

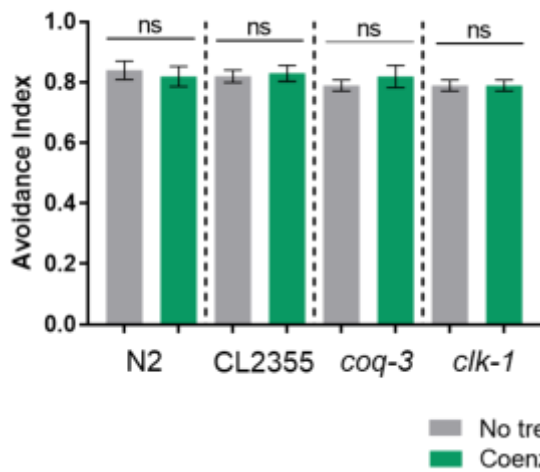


Figure 3.13: Average avoidance index of all strains in both untreated and coenzyme Q<sub>10</sub> treatment conditions at 16°C

not adversely affecting the chemosensory ability of all these strains.

The focus for this assay with this treatment condition was the CL2355 transgenic model at 25°C. This is again due to the fact that this was the only strain to show a decrease in chemosensory ability before treatment at this

temperature condition as can be seen in Figure 3.1. While all the other strains being tested displayed a normal behavioral phenotype of this assay. Thus, it was expected that the N2, *clk-1*, and *coq-3* strains would produce normal values for the avoidance index. The results for this can be seen in Figure 3.14. The wild-type worms (N2) produced a value of  $0.81 \pm 0.0233$  for both

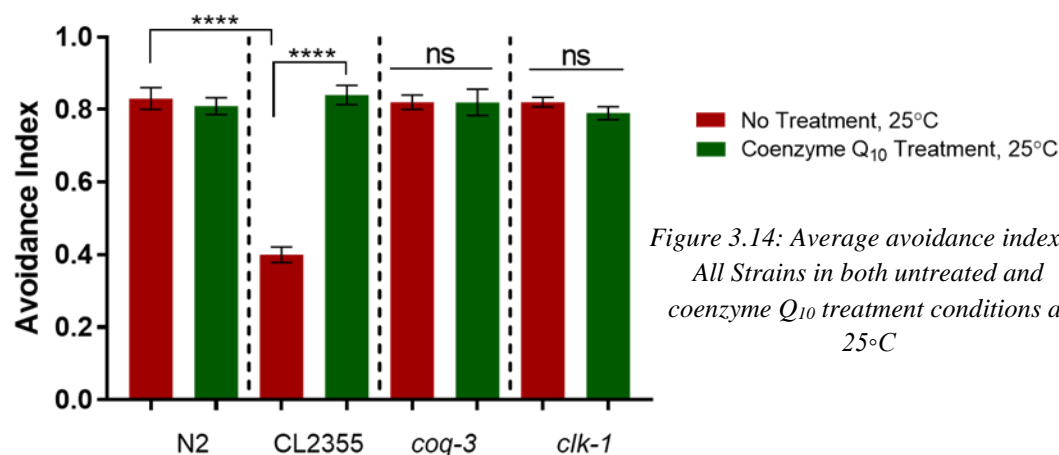


Figure 3.14: Average avoidance index of All Strains in both untreated and coenzyme Q<sub>10</sub> treatment conditions at 25°C

this temperature and treatment condition. The *clk-1* and *coq-3* strains also had similar avoidance index values of  $0.79 \pm 0.0179$

and  $0.82 \pm 0.0359$ . When tested the CL2355 strain produced a value of  $0.83 \pm 0.0260$  ( $p < 0.0001$ ).

This value is approximately the avoidance index value of the wild-type *C. elegans*. This indicates that treatment with coenzyme Q<sub>10</sub> was able to rescue the CL2355's, the pan-neuronal AD model, chemosensory ability. As these worms typically have a significant decrease in avoidance behavior due A $\beta$  plaques that are customarily present, this shows that these plaques are no longer having a detrimental effect due to coenzyme Q<sub>10</sub> treatment. As coenzyme Q<sub>10</sub>

works in the electron transport chain, these results support the claim that energy transduction is altered in Alzheimer's model worms.

### 3.3.2 Chemotaxis Assay

Similar

to the

punicalagin

treatment,

coenzyme Q<sub>10</sub>

treatment was

also used to

measure the

effectiveness in

rescuing

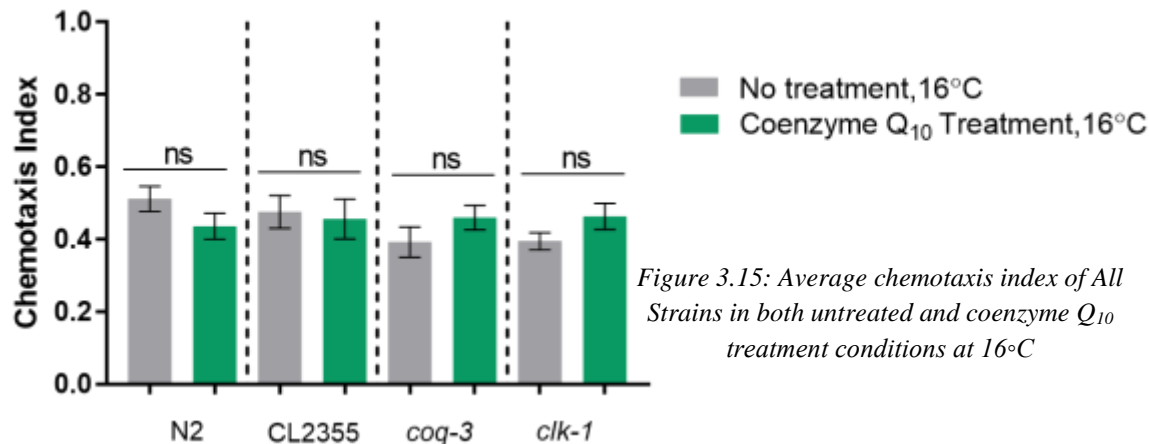


Figure 3.15: Average chemotaxis index of All Strains in both untreated and coenzyme Q<sub>10</sub> treatment conditions at 16°C

chemosensory ability through the chemotaxis assay, these results are available in *Figure 3.15* and *Figure 3.16*. Like the punicalagin treatment, the coenzyme Q<sub>10</sub> was tested as a supplement at both 16°C and 25°C temperature conditions. The wild-type N2 worms again saw a lower chemotaxis index value for 16°C when compared to 25°C. In addition to the decreased chemotaxis index when compared to the N2 worms that did not undergo any treatment. N2 worms being treated with coenzyme Q<sub>10</sub> had a chemotaxis index of  $0.436 \pm 0.0632$  at 16°C and  $0.689 \pm 0.0459$  at 25°C. As hypothesized earlier, the decrease at the lower temperature is likely due to the slowed metabolic processes in the worm, and the slight decrease associated with the treatment is due to giving healthy worms an unnecessary supplement.

The transgenic Alzheimer's Disease worms (CL2355) had an increase in chemotaxis index under both temperature conditions as compared to the same strain that did not undergo treatment. At 16°C the CL2355 strain had a chemotaxis index of  $0.563 \pm 0.0723$  while the 25°C condition had a chemotaxis index of  $0.665 \pm 0.0612$  ( $p=0.0003$ ). The attractive chemosensory ability of the *clk-1* metabolic mutant worms did not seem to be affected by coenzyme Q<sub>10</sub> treatment. At 16°C the chemotaxis index was  $0.453 \pm 0.0710$  and at 25°C the chemotaxis index measured  $0.497 \pm 0.0412$ . The *coq-3* metabolic mutants, however, were positively affected by coenzyme Q<sub>10</sub> treatment, showing the classical full rescue to the wild-type chemotaxis index. At

16°C the worms had a chemotaxis index of  $0.524 \pm 0.0391$  and at 25°C  $0.622 \pm 0.0442$  ( $p=0.0220$ ).

Both metabolic mutants were expected to be rescued by the coenzyme Q<sub>10</sub> treatment as coenzyme Q<sub>10</sub> works directly in the electron transport chain to produce ATP and both mutations

that these worms have are in the production of the coenzyme Q in the electron transport chain.

The *coq-3* mutants acted as expected under the coenzyme Q<sub>10</sub> treatment. The lack of increase in chemotaxis

index was not expected

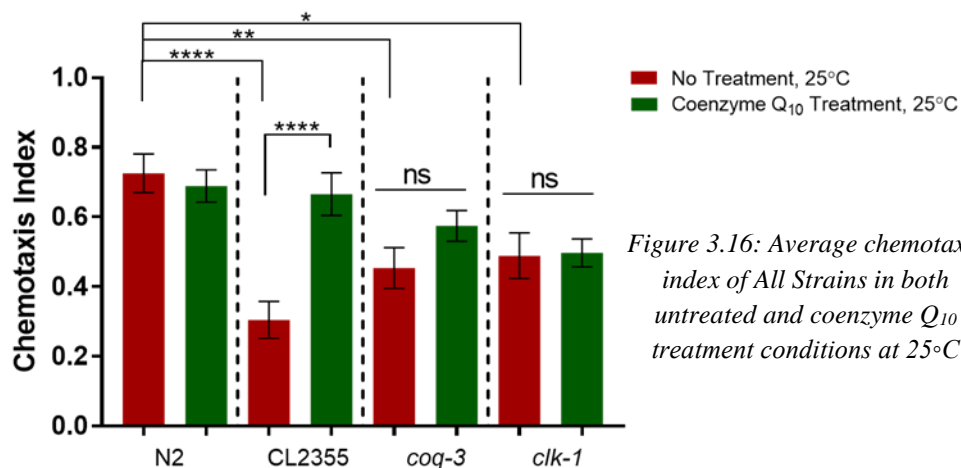


Figure 3.16: Average chemotaxis index of All Strains in both untreated and coenzyme Q<sub>10</sub> treatment conditions at 25°C

for *clk-1* worms. The mutation these worms have occurs in different parts of the coenzyme Q production pathway, and may be bypassed in coenzyme Q production if it is not working properly. The rescue of the CL2355 worms with the coenzyme Q<sub>10</sub> contributes further to our conclusion that Alzheimer's Disease worms have altered ATP production.

### 3.3.3 Mobility Assay

Wild-type N2 worms grown on coenzyme Q<sub>10</sub> were the slowest of all 25°C wild-type trials, at  $73.018 \pm 3.826$   $\mu\text{m/s}$ , and showed no change at 16°C on coenzyme Q<sub>10</sub>, moving at  $77.77 \pm 6.77$   $\mu\text{m/s}$ . As seen in Figure 3.17 and Figure 3.18. This may be due to a possible overloading of energy

transduction

pathways,

specifically in the

electron transport

chain as

coenzyme Q<sub>10</sub> is

an important

factor.

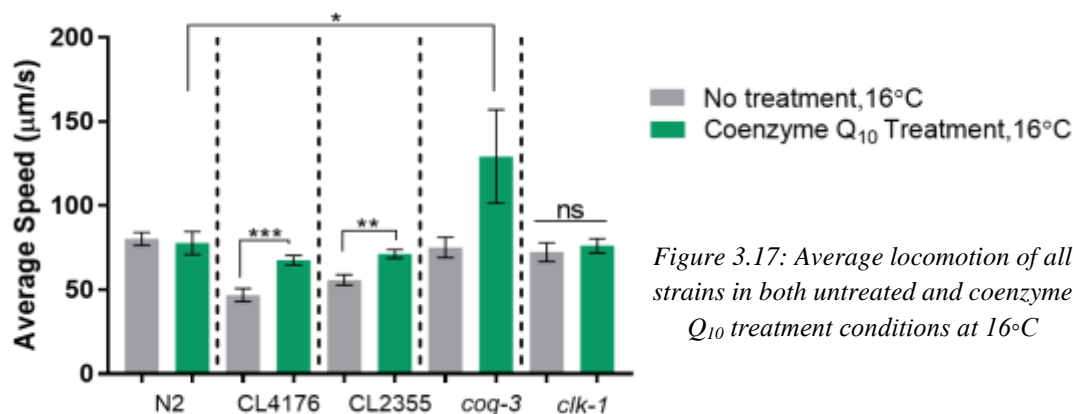


Figure 3.17: Average locomotion of all strains in both untreated and coenzyme Q<sub>10</sub> treatment conditions at 16°C

Supplementation of a healthy working system with a critical enzyme isn't always beneficial--over congestion effects may counteract any AD model benefits of the drug. CL4176 on coenzyme Q<sub>10</sub> showed no change from untreated 25°C trials, at  $37.22 \pm 2.31 \mu\text{m/s}$  ( $p=0.0057$ ), but showed an increase at 16°C from the untreated condition to  $67.64 \pm 2.83 \mu\text{m/s}$  ( $p=0.0004$ ). CL2355 worms grown on coenzyme Q<sub>10</sub> showed a slight decrease to  $44.99 \pm$

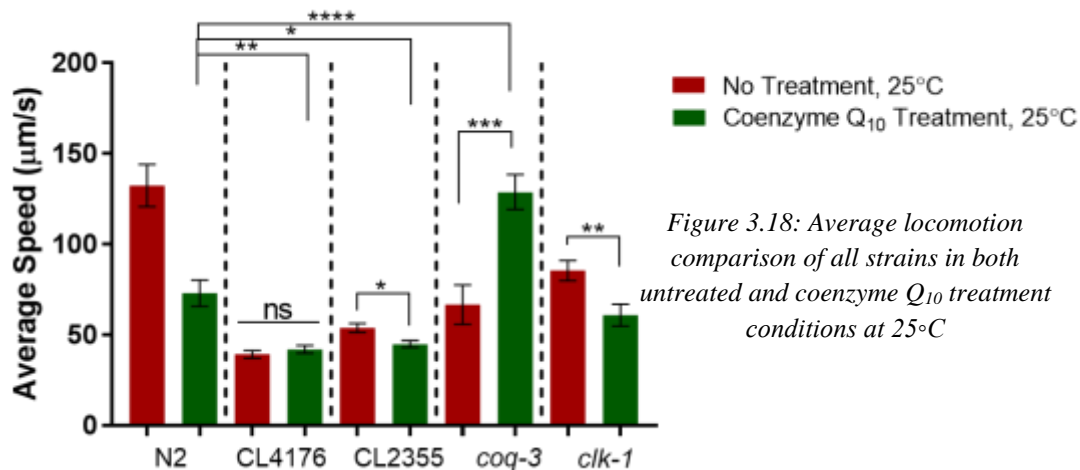


Figure 3.18: Average locomotion comparison of all strains in both untreated and coenzyme Q<sub>10</sub> treatment conditions at 25°C

$1.91 \mu\text{m/s}$  ( $p=0.0104$ ,  $p=0.0136$ ) at 25°C, but like the muscular AD strain showed an increase from the untreated 16°C trials to  $71.30 \pm 2.55 \mu\text{m/s}$  ( $p=0.0012$ ). *Clk-1* metabolic mutants also were not rescued, with a treated speed at 25°C of  $60.98 \pm 6.07 \mu\text{m/s}$  ( $p=0.0080$ ) and an unchanged treated speed at 16°C of  $76.18 \pm 4.30 \mu\text{m/s}$ . This could be because the *clk-1* mutation is further upstream than the main coenzyme Q<sub>10</sub> synthesis protein that is mutated in *coq-3*, which could mean there are further-reaching effects than just a coenzyme Q<sub>10</sub> deficiency. Finally, *coq-3* worms grown on coenzyme Q<sub>10</sub> produced a robust wild-type rescue, with a treated average speed of  $128.82 \pm 9.62 \mu\text{m/s}$  ( $p<0.0001$ ) at 25°C and a surprisingly high speed of  $129.29 \pm 27.72 \mu\text{m/s}$  ( $p=0.0342$ ,  $p=0.0005$ ) at 16°C. This was expected, as *coq-3* worms contain a mutated enzyme that facilitates the biosynthesis of coenzyme Q<sub>10</sub>, and as such can be rescued by simple supplementation with the missing product.

Coenzyme Q<sub>10</sub> was not successful in rescuing mobility in either AD model worm when heatshocked and fully expressing human A $\beta$ . Additionally, it did not rescue *clk-1* worms, possibly because the *clk-1* mutation is further upstream than the main coenzyme Q<sub>10</sub> synthesis protein that is mutated in *coq-3*. This means that there may be further-reaching effects than just a coenzyme Q<sub>10</sub> deficiency. The drug did, however, rescue *coq-3* worms back to wild-type levels. This was expected, as *coq-3* worms contain a mutated enzyme that is directly responsible for the

biosynthesis of coenzyme Q10, and as such can be rescued by supplementation of the missing product.

### 3.3.4 ATP Bioluminescence Assay

Once we observed the results from the behavioral assays treated with coenzyme Q<sub>10</sub>, we then wanted to discover the effects of this supplement on the ATP concentrations in each of the strains. The worms were once again propagated on a plate seeded with OP50 and Coenzyme Q<sub>10</sub> at both temperatures in order to test this. The results for the coenzyme Q<sub>10</sub> treatment at both temperature conditions can be seen in *Figure 3.19 and 3.20*. Many differences were observed for each of the strains once treated with this compound. At both temperatures the wild-type strain was observed to have a large decrease in the ATP concentration when given this treatment. The amount of ATP was measured to  $54.57 \pm 13.7 \mu\text{M}$  at 16°C and  $18.1 \pm 1.123 \mu\text{M}$  at 16°C and 25°C. This data shows that the coenzyme Q<sub>10</sub> treatment significantly decreases the amount of ATP present in these *C. elegans* when compared to their untreated values.

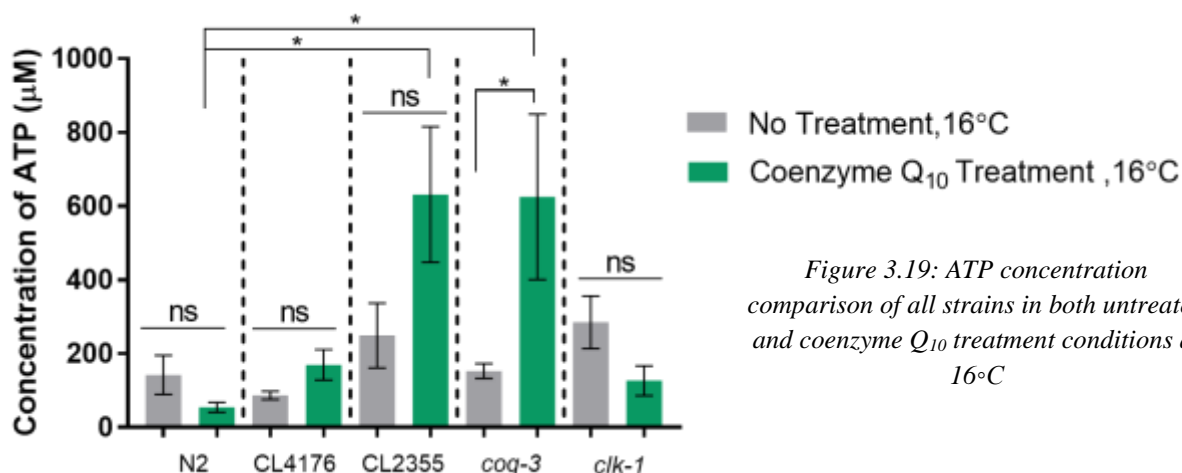


*Figure 3.19: ATP concentration comparison of all strains in both untreated and coenzyme Q<sub>10</sub> treatment conditions at 16°C*

The metabolic mutant data is very peculiar compared to the other data collected. Each mutant had contrasting results at each temperature condition. The *coq-3* worms had a large increase in ATP production at 16°C while at 25°C is significantly decreased. The ATP concentrations were calculated to  $625.6 \pm 224 \mu\text{M}$  and  $35.29 \pm 7.046 \mu\text{M}$  ( $p=0.0079$ ) at 16°C and 25°C. This 16°C data indicates that a significant rise in ATP levels, which is what is expected when given this compound. However, we currently do not have an explanation for the 25°C concentration. This value is very low compared to any of the other values and is unexpected. At the higher temperature we had expected for a significant amount of ATP to be present even though all metabolic process have increased. The only plausible explanation for this

is that the supplement is causing either the ATP production to slowed so much that the process nearly stops or it is over producing so much that it eventually just causes this system to crash. A similar trend

is observed in the *clk-1* mutant. At 16°C, these worms produced an ATP concentration

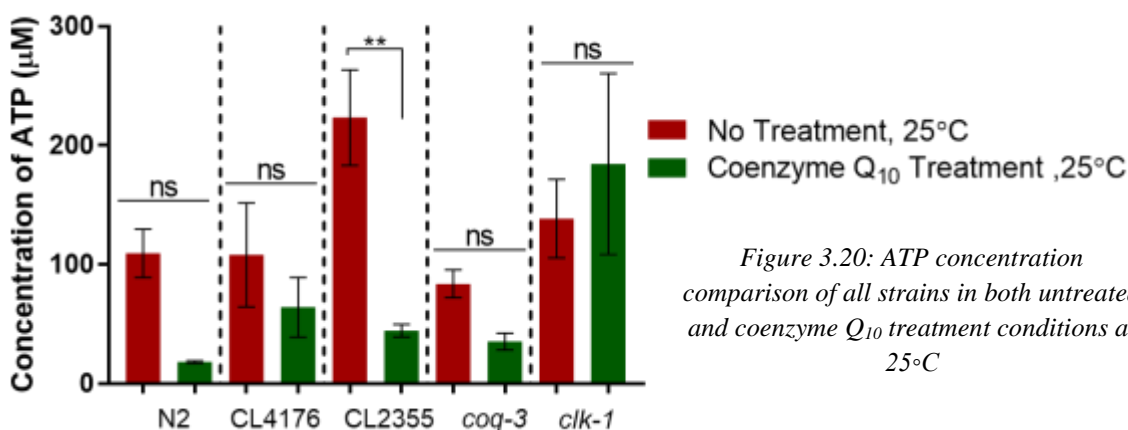


Figure 3.20: ATP concentration comparison of all strains in both untreated and coenzyme Q<sub>10</sub> treatment conditions at 25°C

$126.7 \pm 40.74 \mu\text{M}$ . Conversely, at 25°C the *clk-1* mutants had a measured amount of  $184.4 \pm 76 \mu\text{M}$  ( $p=0.0393$ ). The AD transgenic models produced much different results than the metabolic mutants. At 16°C both strains displayed an increased in the ATP concentration while at 25°C they both decreased when compared to the untreated worms. The CL4176 strain produced a result of  $169.9 \pm 41.3 \mu\text{M}$  at 16°C and  $64.02 \pm 25.48 \mu\text{M}$  at 25°C. The pan-neuronal model produced values that had a similar trend. At 16°C, the CL2355 worms had an ATP concentration of  $631.6 \pm 184 \mu\text{M}$  ( $p=0.0475$ ) while at 25°C this same strain had a measured ATP value of  $44.33 \pm 5.298 \mu\text{M}$  ( $p=0.0013$ ).

The 25°C data is what was expected with this supplement while the 16°C was not. As *clk-1* has a mutation in the electron transport chain, it was completely expected that coenzyme Q<sub>10</sub> would cause them to have increase in ATP levels at both temperature conditions. Even though both of these values are around the untreated wild-type levels, there is no explanation as to why this strain increased under one temperature and decreased under another. However, based on the results it appears that at lower temperatures this compound slows down the ATP production process to a small extent, around what would be observed in untreated conditions. The data shows that when given treatment with coenzyme Q<sub>10</sub> that there is a significant decrease in the amount of ATP when compared to untreated conditions at 25°C. This then indicates that this supplement is able to alleviate the overproduction side effects of the AB plaques. Based on the punicalagin data it would have been expected both of these conditions would decrease as well. However the exact opposite is seen, thus the only plausible explanation for this is that the

supplement treatment is causing the faulty ATP production system to severely increase the amount of ATP in the organism.

## 4. Conclusions and Future Work

### 4.1 Conclusions

The results obtained over the course of this project paint an interesting picture for two potential treatments for Alzheimer's Disease. In this project, three behavioral assays and one biochemical ATP assay were performed on transgenic AD-type and metabolic mutant strains of *C. elegans*. Avoidance and chemotaxis assays were used to test chemosensation while locomotion assays quantified mobility. Through these assays, deficits in chemosensation and locomotion were observed in both AD and metabolic mutant strains, confirming the validity of these assays for the measurement of behavioral phenotypes. Additionally, phenotypic deficits of impaired chemosensation and locomotion in the AD model worms mirror those found in human AD patients, further supporting the use of transgenic AD strains as a model system. Metabolic mutants exhibited significant mobility impairments and showed deficits in the chemotaxis assay, so they served as a suitable counterpart to the AD worms in the comparison of treatment efficacy and mechanism of action. Additionally, the project employed a bioluminescent ATP assay to quantify ATP levels in each strain under non-treated and treated conditions in order to further explore the role of energy transduction in Alzheimer's Disease. All untreated strains showed wild-type levels except for the pan-neuronal AD strain CL2355, which showed a twofold increase in measured ATP levels. This baseline value indicates that ATP production in worms expressing A $\beta$  is much higher than normal, supporting the initial theory of metabolic disruption.

The results obtained in this project also indicate that punicalagin is able to successfully rescue chemotaxis defects due to expression of human A $\beta$  in the pan-neuronal AD strain. Pan-muscular AD worms were not tested in the chemosensory behavioral assays, but showed only a small mobility rescue, as did the pan-neuronal AD worms. This suggests that this treatment is able to partially rescue locomotion, but not fully to wild-type levels. Chemotactic deficits in the metabolic mutants were also rescued to wild-type levels by punicalagin, suggesting that the compound is active in the electron transport chain to some extent. This conclusion is further supported by the locomotion assay results, which showed a partial rescue in *coq-3* and a decrease in mobility in *clk-1*. Although the effects were not necessarily positive, they support the hypothesis that punicalagin has an effect in energy transduction pathways.

ATP bioluminescence assays performed on AD worms treated with punicalagin show a decrease in ATP concentration in both strains. Most notably, pan-neuronal AD worms show a

decrease back to wild-type ATP levels, indicating that punicalagin was able to rescue a normal metabolic phenotype, at least with regards to ATP production. The mechanism of action of punicalagin is not currently known, but it is a known antioxidant. One possible explanation involves the suppression of reactive oxygen species associated with A $\beta$  accumulation and neuronal damage. This falls in line with earlier data; if punicalagin can inhibit harmful effects of A $\beta$  accumulation, it would prevent neuronal degradation and effectively rescue neuronal function and chemotaxis. Additionally, the ATP assays for the metabolic strains showed alternate effects in either strain: *coq-3* increased when treated, and *clk-1* decreased when grown on punicalagin. While the results are not consistent as to punicalagin's effect on the electron transport chain, there is a clear and significant difference between treated and untreated worms, indicating that it has an effect on energy transduction.

Results also indicated that coenzyme Q<sub>10</sub> is able to rescue chemosensation in pan-neuronal AD worms. Both chemotaxis and avoidance assays show a robust wild-type rescue. However, coenzyme Q<sub>10</sub> treatment does not rescue mobility, and actually causes a slight decrease in mobility in neuronal AD worms. The metabolic mutants displayed similar results to the AD model worms, but only showed a defect in the chemotaxis assay and mobility assays, and not the avoidance assay. However, neither strain of metabolic mutants was able to be rescued in the chemotaxis assay. This indicates that coenzyme Q<sub>10</sub> may not be directly involved in neuronal signaling, but is somehow involved in mediating the effects of neurodegeneration in A $\beta$ -expressing neurons. ATP data obtained for coenzyme Q<sub>10</sub> showed the same effects as punicalagin in the pan-neuronal AD strain. ATP levels were again reduced from twice wild-type values to wild-type levels. Coenzyme Q<sub>10</sub> is a known coenzyme in the electron transport chain, so this may indicate that the electron transport chain is directly involved in effecting the Alzheimer's Disease phenotype in *C. elegans*. ATP values for metabolic mutants returned strange values, as *coq-3* ATP levels decrease and *clk-1* levels increased when treated. Coenzyme Q<sub>10</sub> is deficient in both mutants, but doesn't necessarily cause a return to wild-type ATP levels. This is due to the fact that the measured values of ATP don't tell the whole story.

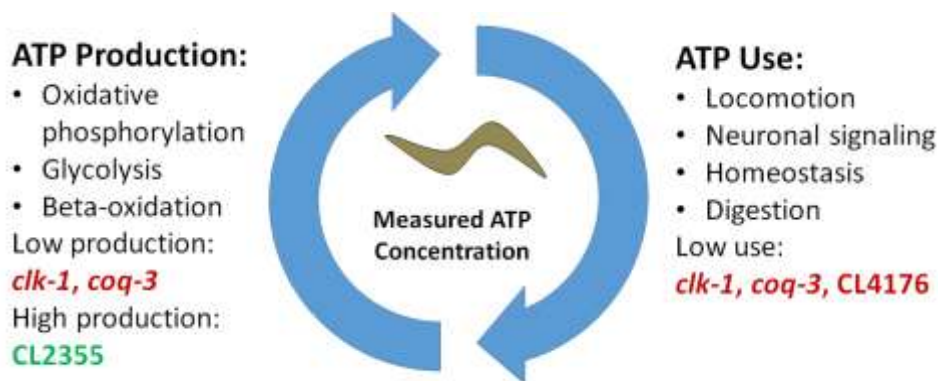


Fig. 4.1: Conceptual understanding of ATP bioluminescence assays

The ATP data obtained illuminated a part of energy transduction in the transgenic AD worms. Measured ATP concentrations show an instantaneous state of the system, which is normally in a dynamic equilibrium in live worms. This equilibrium, as can be seen in *Figure 4.1* above, is a function of both ATP production rates and ATP usage rates. The N2 worms provided a baseline ATP concentration in healthy worms. The metabolic worms both exhibited decreased ATP production, however, their ATP concentration was equal to the wild type as these worms seem to have an adapted equilibrium, balancing low ATP production with low use through slowed movements. These worms use less ATP, as exhibited in the behavioral assays, to maintain a healthy ATP homeostasis. In the behavioral assays, the CL2355 worms also exhibited decreased ATP usage, but in the ATP bioluminescence assay, the same worms had a significantly higher concentration of ATP. These worms did not have an increased ATP use to couple their increased ATP production, causing a disrupted ATP equilibrium. The use of the bioluminescence assay provided us with information to understand how ATP is being produced and processed in *C. elegans* models of Alzheimer's Disease.

## 4.2 Future Work

The research conducted yielded a deeper understanding on the metabolic homeostasis that regulates ATP levels in the Alzheimer's Disease worm models. Additionally, more work needs to be done to continue to uncover all of the changes that occur in the metabolism of Alzheimer's Disease in this *C. elegans* model. To accomplish this, a comprehensive metabolic analysis needs to be performed. The ATP bioluminescence assays gave us a glimpse of the ATP concentration in the entirety of the worm at a specific time. The metabolic analysis should look at worms under different conditions that would affect energy uses. Different metabolites, including NADH and

FADH<sub>2</sub> should be studied to build a larger picture of energy transduction in Alzheimer's Disease. The metabolite analysis should be adapted from the ATP bioluminescence assay to focus more specifically on the mitochondria in neurons, as opposed to entire worm lysate. This process could be difficult in worms due to their size, so a different model organism would need to be considered. Finding a way to perform this type of assay successfully will allow energy in neurons of Alzheimer's Disease patients to be better characterized. From this research, more information on the mechanisms of each treatment could be gathered to allow for further understanding on the metabolism in AD.

Punicalagin and Coenzyme Q<sub>10</sub> were able to rescue both attractive and aversive chemosensory ability in the Alzheimer's Disease model *C. elegans* strains. We only tested the treatments at one concentration and as a dietary supplement that the worms were constantly exposed to. To further understand both punicalagin and coenzyme Q<sub>10</sub>'s effectiveness in alleviating symptoms of Alzheimer's Disease there are multiple future projects that can be completed to learn more. One would be to vary the concentration in order to see the upper and lower limits of each supplement that can produce a phenotypic rescue. The same behavioral assays could be used at a variety of higher and lower concentrations. Additionally, both supplements should be tested as both a symptomatic and a restorative treatment options. This could also be completed using the same assays but adapting to test the same worms multiple times. For preventative treatment, the worms would be exposed to the punicalagin from the start and behavior would be analyzed, as done in this study. After the first behavior analysis, worms would then be moved to an untreated plate for 1-2 days and then tested again. For restorative treatment, worms would be grown on non-treated plates to adulthood and then tested for behavior. After this baseline testing, they would be given a treatment for 1-2 days and retested.

Additionally, neither of the treatments were successful at treating the deficit in the mobility phenotype in the AD model *C. elegans*. There could be other polyphenols and other dietary supplements that could induce aid in mobility. There is more research that suggests potential therapeutics in terms of mobility restoration. Additionally, the further metabolite analysis mentioned previously could help lead to the discovery of a potential therapeutic. Testing of the mobility in *C. elegans* could also be furthered analyzed using the different methods available in the Worm Tracker software, including thrashing, reversals, general orientation/pathfinding, and turning frequency, to better test potential treatments

## Bibliography

- Abbas, M., Saeed, F., Anjum, F. M., Afzaal, M., Tufail, T., Bashir, M. S., . . . Suleria, H. A. R. (2017). Natural polyphenols: An overview. *International Journal of Food Properties*, 20(8), 1689-111. 10.1080/10942912.2016.1220393 Retrieved from <http://www.tandfonline.com/doi/abs/10.1080/10942912.2016.1220393>
- Alberts, B., Johnson, A., Lewis, J., Raff, M., Roberts, K., & Walter, P. (2002). *Molecular biology of the cell* (Fourth ed.) Garland Science. Retrieved from <https://www.ncbi.nlm.nih.gov/books/NBK26904/>
- Alexander, A. G., Marfil, V., & Li, C. (2014). Use of caenorhabditis elegans as a model to study alzheimer's disease and other neurodegenerative diseases. *Frontiers in Genetics*, 5, 279. Retrieved from <http://www.ncbi.nlm.nih.gov/pubmed/25250042>
- Anandhan, A., Jacome, M. S., Lei, S., Hernandez-Franco, P., Pappa, A., Panayiotidis, M. I., . . . Franco, R. (2017). Metabolic disorder dysfunction in parkinson's disease: Bioenergetics, redox homeostasis and central carbon metabolism. *Brain Research Bulletin*, 10.1016/j.brainresbull.2017.03.009 Retrieved from <https://www.clinicalkey.es/playcontent/1-s2.0-S036192301730165X>
- Anhê, F. F., Desjardins, Y., Pilon, G., Dudonné, S., Genovese, M. I., Lajolo, F. M., & Marette, A. (2013). Polyphenols and type 2 diabetes: A prospective review. *PharmaNutrition*, 1(4), 105-114. 10.1016/j.phanu.2013.07.004 Retrieved from <http://www.sciencedirect.com/science/article/pii/S2213434413000406>
- Begley, P., Xu, J., Church, S., Reid, S., Kim, E., Curtis, m., . . . Cooper, G. (2016). Metabolite mapping reveals sever widespread&nbsp;perturbation of multiple metabolic processes in huntington's disease human brain&nbsp; *Molecular Basis of Disease*,
- Berg, J. M., Tymoczko, J. L., & Stryer, L. (2002). *Biochemistry* (Fifth ed.) W H Freeman. Retrieved from <https://www.ncbi.nlm.nih.gov/books/NBK22448/>
- Bhullar, K. S., & Rupasinghe, H. P. V. (2013). Polyphenols: Multipotent therapeutic agents in neurodegenerative diseases. Retrieved from <https://www.hindawi.com/journals/omcl/2013/891748/>

- Brutsaert, E. (2017). Diabetes mellitus (DM) - endocrine and metabolic disorders. Retrieved from <https://www.merckmanuals.com/professional/endocrine-and-metabolic-disorders/diabetes-mellitus-and-disorders-of-carbohydrate-metabolism/diabetes-mellitus-dm>
- Burn, A., Burns, R., & Patterson, M. *Gender-based differences in parkinson's disease and amyotrophic lateral sclerosis expression in C. elegans* &nbsp;.
- C. elegans as a model organism: An introduction. Retrieved from <http://modencode.sciencemag.org/worm/introduction/>
- CAENORHABDITIS elegans AS A GENETIC ORGANISM. (2006). Retrieved from <http://www.wormatlas.org/ver1/handbook/anatomyintro/anatomyintro.htm>
- Clk-1 (gene). (2007). Retrieved from [http://www.wormbase.org/species/c\\_elegans/gene/WBGene00000536#0-9g-3](http://www.wormbase.org/species/c_elegans/gene/WBGene00000536#0-9g-3)
- Coq-3 (gene). Retrieved from [http://www.wormbase.org/species/c\\_elegans/gene/WBGene00000763#0-9g-3](http://www.wormbase.org/species/c_elegans/gene/WBGene00000763#0-9g-3)
- Coyle, V., Nikolaki, V., & Ong, F. *The effects of punicalagin and tannic acid on caenorhabditis elegans models of alzheimer's disease.*
- Dostal, V., & Link, C. D. (2010). Assaying  $\beta$ -amyloid toxicity using a transgenic C. elegans model. *Journal of Visualized Experiments*, (44), 2252.
- Elizabeth Moreno-Arriola, Noemí Cárdenas-Rodríguez, Elvia Coballase-Urrutia, José Pedraza-Chaverri, Liliana Carmona-Aparicio, & Daniel Ortega-Cuellar. (2014). Caenorhabditis elegans: A useful model for studying metabolic disorders in which oxidative stress is a contributing factor. *Oxidative Medicine and Cellular Longevity*, 2014, 1-9. 10.1155/2014/705253 Retrieved from <http://dx.doi.org/10.1155/2014/705253>
- Falk, M. J., Zhang, Z., Rosenjack, J. R., Nissim, I., Daikhin, E., Sedensky, M. M., . . . Morgan, P. G. (2008). Metabolic pathway profiling of mitochondrial respiratory chain mutants in C. elegans. *Molecular Genetics and Metabolism*, 93(4), 388-397. 10.1016/j.ymgme.2007.11.007 Retrieved from <https://www.sciencedirect.com/science/article/pii/S1096719207005963>
- Gawain McColl, Blaine R. Roberts, Adam P. Gunn, Keyla A. Perez, Deborah J. Tew, Colin L. Masters, . . . Ashley I. Bush. (2009). The caenorhabditis elegans model A $\beta$ <sub>1-42</sub> of alzheimer

- disease predominantly expresses A $\beta$ <sub>3-42</sub>. *Journal of Biological Chemistry*, 284(34), 22697. 10.1074/jbc.C109.028514 Retrieved from <http://www.jbc.org/content/284/34/22697.abstract>
- Graef, J. W., Wolfsdorf, J. I., & Greenes, D. S. (2008). *Manual of pediatric therapeutics* Lippincott Williams & Wilkins.
- Hilliard, M. A., Bargmann, C. I., & Bazzicalupo, P. (2002). *C. elegans* responds to chemical repellents by integrating sensory inputs from the head and the tail. *Current Biology*, 12(9), 730-734. 10.1016/S0960-9822(02)00813-8 Retrieved from <http://www.sciencedirect.com/science/article/pii/S0960982202008138>
- Huan Cai, Wei-na Cong, Sunggoan Ji, Sarah Rothman, Stuart Maudsley, & Bronwen Martin. (2012). Metabolic dysfunction in alzheimers disease and related neurodegenerative disorders. *Current Alzheimer Research*, 9(1), 5-17. Retrieved from <http://www.eurekaselect.com/openurl/content.php?genre=article&issn=15672050&volume=9&issue=1&spage=5>
- Jin, J. (2015). Alzheimer's disease. Retrieved from <https://jamanetwork.com/journals/jama/fullarticle/2247146>
- Jonckheere, A. I., Smeitink, J. A. M., & Rodenburg, R. J. T. (2012). Mitochondrial ATP synthase: Architecture, function and pathology. *Journal of Inherited Metabolic Disease*, 35(2), 211-225. 10.1007/s10545-011-9382-9 Retrieved from <http://www.narcis.nl/publication/RecordID/oai:repository.ubn.ru.nl:2066%2F108684>
- Kaletta, T., & Hengartner, M. O. (2006). Finding function in novel targets: *C. elegans* as a model organism. *Nature Reviews Drug Discovery*, 5(5), 387-399. 10.1038/nrd2031 Retrieved from <http://dx.doi.org/10.1038/nrd2031>
- L Ryan Baugh. (2013). To grow or not to grow: Nutritional control of development during *caenorhabditis elegans* L1 arrest. *Genetics*, 194(3), 539-555. 10.1534/genetics.113.150847 Retrieved from <http://www.ncbi.nlm.nih.gov/pubmed/23824969>
- Latest alzheimer's facts and figures. (2013). Retrieved from <https://alz.org/facts/overview.asp>
- Lee, R. Y. N., Hench, J., & Ruvkun, G. (2001). Regulation of *C. elegans* DAF-16 and its human ortholog FKHL1 by the *daf-2* insulin-like signaling pathway. *Current Biology*, 11(24),

- 1950-1957. 10.1016/S0960-9822(01)00595-4 Retrieved from  
<https://www.sciencedirect.com/science/article/pii/S0960982201005954>
- Lublin, A. L., & Link, C. D. (2013). Alzheimer's disease drug discovery: In vivo screening using caenorhabditis elegans as a model for  $\beta$ -amyloid peptide-induced toxicity. *Drug Discovery Today. Technologies*, 10(1), e115. Retrieved from  
<http://www.ncbi.nlm.nih.gov/pubmed/24050239>
- Manach, C., Scalbert, A., Morand, C., Rémésy, C., & Jiménez, L. (2004). Polyphenols: Food sources and bioavailability. *The American Journal of Clinical Nutrition*, 79(5), 727-747. 10.1093/ajcn/79.5.727 Retrieved from  
<https://academic.oup.com/ajcn/article/79/5/727/4690182>
- Mango, S. E. (2007). The C. elegans pharynx: A model for organogenesis. *WormBook : The Online Review of C. Elegans Biology*, , 1. 10.1895/wormbook.1.129.1 Retrieved from  
<http://www.ncbi.nlm.nih.gov/pubmed/18050503>
- Markaki, M., & Tavernarakis, N. (2010). Modeling human diseases in caenorhabditis elegans. *Biotechnology Journal*, 5(12), 1261-1276. 10.1002/biot.201000183 Retrieved from  
<http://www.ncbi.nlm.nih.gov/pubmed/21117084>
- Nakamoto, R. K., Baylis Scanlon, J. A., & Al-Shawi, M. K. (2008). The rotary mechanism of the ATP synthase. *Archives of Biochemistry and Biophysics*, 476(1), 43-50. 10.1016/j.abb.2008.05.004 Retrieved from  
<https://www.sciencedirect.com/science/article/pii/S0003986108002531>
- Okuno, D., Iino, R., & Noji, H. (2011). Rotation and structure of FoF1-ATP synthase. *The Journal of Biochemistry*, 149(6), 655-664. 10.1093/jb/mvr049 Retrieved from  
<https://academic.oup.com/jb/article/149/6/655/2182760>
- Olajide, O., Kumar, O., Velagapudi, R., Okorji, U., & Fiebich, B. (2014). Punicalagin inhibits neuroinflammation in LPS-activated rat primary microglia. *Molecular Nutrition and Food Research*, Retrieved from <https://onlinelibrary.wiley.com/doi/abs/10.1002/abstract>
- Olichney, J. M., Murphy, C., Hofstetter, C. R., Foster, K., Hansen, L. A., Thal, L. J., & Katzman, R. (2005). Anosmia is very common in the lewy body variant of alzheimer's disease.

- Journal of Neurology, Neurosurgery, and Psychiatry*, 76(10), 1342-1347.  
10.1136/jnnp.2003.032003 Retrieved from <http://www.ncbi.nlm.nih.gov/pubmed/16170073>
- Palikaras, K., & Tavernarakis, N. (2016). Intracellular assessment of ATP levels in *Caenorhabditis elegans*. *Bio-Protocol*, 6(23)10.21769/BioProtoc.2048 Retrieved from <https://www.ncbi.nlm.nih.gov/pmc/articles/PMC5303341/>
- Price, J. L., & Morris, J. C. (1999). Tangles and plaques in nondemented aging and "preclinical" Alzheimer's disease. *Annals of Neurology*, 45(3), 358. Retrieved from <http://www.ncbi.nlm.nih.gov/pubmed/10072051>
- Rebecca C. Brown, Alan H. Lockwood, & Babasaheb R. Sonawane. (2005). Neurodegenerative diseases: An overview of environmental risk factors. *Environmental Health Perspectives*, 113(9), 1250-1256. 10.1289/ehp.7567 Retrieved from <http://www.jstor.org/stable/3436426>
- Saba, L. (2015). *Imaging in neurodegenerative disorders* (1. ed. ed.). Oxford: Oxford Univ. Press.
- Senior, A. E., Nadanaciva, S., & Weber, J. (2002). The molecular mechanism of ATP synthesis by F1F0-ATP synthase. *Biochimica Et Biophysica Acta (BBA) - Bioenergetics*, 1553(3), 188-211. 10.1016/S0005-2728(02)00185-8 Retrieved from <http://www.sciencedirect.com/science/article/pii/S0005272802001858>
- Silke Fuchs, Jacob G Bundy, Sarah K Davies, Jonathan M Viney, Jonathan S Swire, & Armand M Leroi. (2010). A metabolic signature of long life in *Caenorhabditis elegans*. *BMC Biology*, 8(1), 14. 10.1186/1741-7007-8-14 Retrieved from <http://www.ncbi.nlm.nih.gov/pubmed/20146810>
- Stiernagle, T. (2006). Maintenance of *C. elegans*. *WormBook : The Online Review of C. Elegans Biology*, , 1. 10.1895/wormbook.1.101.1 Retrieved from <http://www.ncbi.nlm.nih.gov/pubmed/18050451>
- Taubert, S. (2016a). *Caenorhabditis elegans* gets metabolic network models. *Cell Systems*, 2(5), 293. Retrieved from <http://www.ncbi.nlm.nih.gov/pubmed/27228345>
- Taubert, S. (2016b). *Caenorhabditis elegans* gets metabolic network models. *Cell Systems*, 2(5), 293. Retrieved from <http://www.ncbi.nlm.nih.gov/pubmed/27228345>

- Use of caenorhabditis elegans as a model to study alzheimer's disease and other neurodegenerative diseases. (2014). Retrieved from <http://scholar.aci.info/view/1478c8ea4f10953012d/148475559ef35aa014d>
- Vauzour, D. (2012). Dietary polyphenols as modulators of brain functions: Biological actions and molecular mechanisms underpinning their beneficial effects. *Oxidative Medicine and Cellular Longevity*, 2012, 914273. Retrieved from <http://www.ncbi.nlm.nih.gov/pubmed/22701758>
- Verma, A. (2014). *Animal biotechnology* (1. publ. ed.). Amsterdam [u.a.]: Elsevier, Academic Press.
- Voet, J., Voet, D., & Pratt, C. (2012). *Fundamentals of biochemistry*; (Fourth ed.). Hoboken, New Jersey: John Wiley & Sons, Inc.
- Wildman, R., & Medeiros, D. (2015). *Advanced human nutrition*; (Third ed.) Jones and Bartlett Publishing.
- Wilson disease. Retrieved from <https://www.niddk.nih.gov/health-information/liver-disease/wilson-disease>
- Wilson's disease - symptoms and causes. (a). Retrieved from <http://www.mayoclinic.org/diseases-conditions/wilsons-disease/symptoms-causes/syc-20353251>
- Yanjue Wu, & Yuan Luo. (2005). Transgenic C. elegans as a model in alzheimers research. *Current Alzheimer Research*, 2(1), 37-45. 10.2174/1567205052772768 Retrieved from <http://www.eurekaselect.com/openurl/content.php?genre=article&issn=15672050&volume=2&issue=1&spage=37>
- Yasuda, R., Noji, H., Kinosita, K., & Yoshida, M. (1998). The rotary machine in the cell, ATP synthase; *Cell*, 93(7), 1117-1124. 10.1016/S0092-8674(00)81456-7 Retrieved from <http://www.jbc.org/content/276/3/1665>
- Yilmaz, L. ., & Walhout, A. M. (2016). A caenorhabditis elegans genome-scale metabolic network model. *Cell Systems*, 2(5), 297-311. 10.1016/j.cels.2016.04.012 Retrieved from <https://www.sciencedirect.com/science/article/pii/S240547121630120X>